The metabolism of nitrogen assimilation in *Medicago truncatula*: a quest for sensors and regulators

José Nuno Leitão

July 2012

UNIVERSIDADE DO PORTO

INSTITUTO DE CIÊNCIAS BIOMÉDICAS ABEL SALAZAR

FACULDADE DE ENGENHARIA

INSTITUTO DE BIOLOGIA MOLECULAR E CELULAR

The metabolism of nitrogen assimilation in *Medicago truncatula*: a quest for sensors and regulators

JOSÉ NUNO DE ARAÚJO LEITÃO

Dissertação de Mestrado em Bioengenharia - Ramo Biotecnologia Molecular

2012

UNIVERSIDADE DO PORTO

INSTITUTO DE CIÊNCIAS BIOMÉDICAS ABEL SALAZAR

FACULDADE DE ENGENHARIA

INSTITUTO DE BIOLOGIA MOLECULAR E CELULAR

The metabolism of nitrogen assimilation in *Medicago truncatula*: a quest for sensors and regulators

JOSÉ NUNO DE ARAÚJO LEITÃO

Dissertação de Mestrado em Bioengenharia - Ramo Biotecnologia Molecular

Aprovado em provas públicas a 23 de julho de 2012 pelo Júri:

Presidente: Alexandre Quintanilha (ICBAS-UP)

Arguente: Mariana Sottomayor (FCUP-UP)

Orientador: Maria Helena Carvalho (IBMC-UP)

2012

«The most exciting phrase to hear in Science,

the one that heralds the most discoveries,

is not “Eureka!” *but* “That’s funny…”*.*

Isaac Asimov

Abstract

The availability of nitrogen (N) is a major factor limiting plant growth and, from this perspective, a fundamental knowledge of the biology of N assimilation is indispensable. In this work, we aimed at analysing the potential of sensors and regulators of the metabolism of N, by focusing on three genes that had been shown to vary significantly in response to the inhibition of Glutamine Synthetase (GS), a central enzyme is this metabolic network. Specifically, the genes assayed were an ammonium transporter (*MtAMT3*), a putative nitrate reductase (*MtNR3*) and a potential transcription factor, *NIN-like protein 7* (*MtNLP7*).

Transcriptomic analysis showed that *MtAMT3* is specific to roots and nodules and *MtNR3* is only expressed in nodules, which is intriguing, given that nitrate is not an N source in this organ. The expression of *MtNLP7* was found to vary in response to the N status.

Through RT-qPCR, in situations where N_2 fixation is impaired, an upregulation of all three genes was seen in Fix^- nodules, yet *MtAMT3* and *MtNR3*, but not of *MtNLP7*, were downregulated in nodules subjected to nitrate treatment. In the context of nodule metabolism, this stimulates the hypotheses that MtAMT3 is the currently unidentified symbiotic ammonium transporter and that MtNR3 is involved in a NO_3^--NO respiration process and/or in the production of nitric oxide.

In three-week old seedlings, *MtNLP7* is induced by NO_3^- and repressed by NH_4^+ at 3 hours of treatment, but at 24 hours it is induced by NH_4^+. The variations observed in *MtNLP7* place it in a central position in N metabolism. The response of GS genes was also screened, but further studies are required to fully understand its regulation by inorganic N.

Together, these data provide new evidence for the potential of *MtAMT3*, *MtNR3* and *MtNLP7* as modulators of the N status within the cell and show their response and that of the GS gene family to differential N provision. Nutrients are now seen as potential signalling molecules and this study provides novel insights as to how plants curb growth, development and activity in response to fluctuating environmental conditions.

Key words: N metabolism; sensor; regulator; *MtAMT3*; *MtNR3*; *MtNLP7*; fixation; symbiosis; *Medicago truncatula*.

Resumo

O azoto (N) é o principal nutriente limitante para o crescimento das plantas e, como tal, um conhecimento da biologia fundamental do N é indispensável. Neste trabalho, procurou-se analisar o potencial de possíveis sensores e reguladores de N, focando em três genes cuja expressão variou significativamente em resposta à inibição da Glutamina Sintetase, uma enzima central nesta rede metabólica, nomeadamente um transportador de amónio (*MtAMT3*), uma possível nitrato reductase (*MtNR3*) e um possível fator de transcrição, *NIN-like protein 7* (*MtNLP7*).

Uma análise do perfil transcriptómico destes genes mostrou que a expressão de *MtAMT3* está limitada a raízes e nódulos e que a expressão de *MtNR3* é ainda mais restrita, estando presente unicamente em nódulos, o que é curioso, dado que neste órgão o nitrato não é uma fonte de N. Verificou-se ainda que a expressão de *MtNLP7* varia em resposta a diferentes condições de N.

Por RT-qPCR, em situações nas quais a fixação de N não está funcional, observou-se a sobre-expressão dos três genes em nódulos Fix^-, enquanto *MtAMT3* e *MtNR3*, mas não *MtNLP7*, estavam subexpressos em nódulos tratados com nitrato. Estas observações, no contexto particular do metabolismo dos nódulos, estimulam as hipóteses que MtAMT3 seja o transportador de amónio do simbiossoma, que até ao momento ainda não foi identificado, e que MtNR3 esteja envolvido num processo respiratório NO_3^--NO e/ou na produção de óxido nítrico.

Em plântulas com três semanas, a expressão de *MtNLP7* é induzida pelo NO_3^- e inibida por NH_4^+ às 3 horas de tratamento, mas induzido por NH_4^+ passado 24 horas. As variações observadas colocam este gene numa posição central no metabolismo do azoto. A resposta dos genes da GS foi também analisada, mas mais estudos são necessários para compreender cabalmente a sua regulação pelo N inorgânico.

Em conjunto, estes dados ilustram o potencial de *MtAMT3*, *MtNR3* e *MtNLP7* enquanto moduladores do *status* de N na célula e descrevem as suas respostas, bem como as dos genes da GS, a uma nutrição diferencial de N. Os nutrientes são agora considerados potenciais moléculas de sinalização e este estudo fornece novas perspetivas sobre o modo como as plantas modulam o crescimento, desenvolvimento e atividade em resposta a flutuações das condições ambientais.

Palavras-chave: Metabolismo de N; sensor; regulador; *MtAMT3*; *MtNR3*; *MtNLP7*; fixação; simbiose; *Medicago truncatula*.

Agradecimentos

À Doutora Helena Carvalho, por me ter dado a conhecer o mundo das plantas, por depois me ter aceitado no seu grupo e por ter embarcado neste projeto. Obrigado pelos seus ensinamentos e pela perspetiva sob a qual vê a Ciência como esta deveria ser: objetiva, cega e desinteressada.

À Ana Rita e à Liliana, que me socorram tantas vezes quando não sabia nada e que continuaram a fazê-lo quando já sabia alguma coisa. Obrigado pelos vossos conselhos práticos, pelo vosso interesse, pela vossa paciência e pela vossa ajuda.

Ao Zé Pedro "Ponto", à Andreia e ao Gil, pelos almoços no sítio do costume, que sempre serviram para debater tudo e mais alguma coisa, desde profundas conversas filosóficas entre um bacalhau com natas, às mais inúteis discussões à mesa com "arroz de aves". À Catarina, pelos lanches nos intervalos das incubações, em que barafustávamos com tudo e com nada. A todos, obrigado pela amizade, pelos bons tempos e pelos conselhos.

A todos os professores que me acompanharam até hoje, sem os quais não poderia ter chegado a este ponto. Pelos ensinamentos, pelo exemplo e por sempre manterem a minha vontade de aprender acesa, muito obrigado.

Aos meus colegas do MIB de 2007-2012, com quem também aprendi imenso, por criarem um ambiente propício ao companheirismo, à amizade, à aprendizagem e à entreajuda.

Aos meus amigos de sempre, aos amigos da AEICBAS e aos amigos da AEGEE, pelos jantares, pelos passeios, pelas viagens, pelas festas, pelas conversas, pelos cafés, por todos os momentos que, de uma forma ou de outra, também me permitem estar aqui.

Aos meus pais e ao meu irmão que me apoiaram, incentivaram (e patrocinaram) nesta aventura da Bioengenharia.

Table of contents

Figure Index

Table Index

Abbreviations and acronyms

A. rhizogenes	*Agrobacterium rhizogenes*
A. thaliana	*Arabidopsis thaliana*
ATP	Adenosine triphosphate
bp	Base-pair
Cb	Cytochrome b
C_q	Quantification cycle
DI	Dimer interface
dpi	Days post infection
dsRNA	Double-stranded RNA
E	Amplification Efficiency
FAD	Flavin adenine dinucleotide
GFP	Green Fluorescent Protein
Gln	Glutamine
Glu	Glutamate
GOGAT	Glutamine-2-oxoglutarate aminotransferase
GS	Glutamine synthetase
HATS	High-affinity ammonium transport system
IPTG	Isopropyl β-D-thiogalactopyranoside
LATS	Low-affinity ammonium transport system
M. truncatula	*Medicago truncatula*
Mo-MPT	Mo-Molybdopterin
*Mt*GEA	*Medicago truncatula* Gene Expression Atlas
N	Nitrogen
NAA	1-Naphthaleneacetic acid
NADH	Nicotinamide adenine dinucleotide
NES	Nuclear export signal
NF	Nod factor
NOS	NO synthase
NR	Nitrate Reductase

PB1	Phox and Bem1
PCR	Polymerase chain reaction
PPT	Phosphinothricin
qPCR	Quantitative real-time PCR
RISC	RNA-induced Silencing Complex
RNAi	RNA interference
S. medicae	*Sinorhizobium medicae*
S. meliloti	*Sinorhizobium meliloti*
siRNA	Small interfering RNA
SMART	Simple Modular Architecture Research Tool
UTR	Untranslated region
Xgal	5-bromo-4-chloro-3-indolyl-beta-D-galactopyranoside

Chapter I

Introduction

In 2011 the world population reached 7 billion people. This unprecedented value is continuously increasing and is expected to reach 9.3 billion by 2050 (*World Population Prospects*, 2011). Never before has humanity been faced with the challenge of feeding and providing shelter, clothes and renewable energy to such a high number of people, especially in a time when the necessity of ensuring environmental sustainability has been acknowledged. What are the solutions to these global challenges? How can we tackle these problems? Do plants exert a paramount part of the equation?

Plants are one of the most important and fascinating groups of living organisms. They harness light from the Sun, supplying Earth with energy and serving as primary producers. They and their ancestors created an oxygen-rich atmosphere through the process of photosynthesis, which enabled the spread of life beyond the oceans and maintains it today. Plants have literally sculpted the very surface of the planet and they drove the evolution of all animals, including our own ancestors. In fact, primates' ability to see the colour red stems from the need to identify ripe fruit. These organisms evolved in ingenious ways to face the challenges with which they came across and are a vital and essential part of the ecosystems, exerting unique functions in the biogeochemical cycles and providing the habitats for biodiversity.

Besides their biological importance, plants also exert a marked socio-economic impact. First, they form the basis of the food supply and provide a source of many industrial and medicinal products. Additionally, plants are also the origin of fossil fuels, but might play a role in the search of alternative energy sources as well. Engineering plants for biofuel production, phytoremediation, herbicide and pest resistance, drought and salt tolerance or increased yield are opportunities continuously offered by plant biotechnology. The concept of molecular pharming is yet another possibility and has been held as a promise of an improved methodology for the economically feasible production of pharmaceuticals, making them

available at a global scale, through the reprogramming of common crop plants with recombinant DNA techniques (Miller, 2003; Paul *et al.*, 2011).

When both the biological and socio-economic impact of plants is considered, the importance of having a fundamental knowledge of plant biology becomes clear and so does the potential that it holds when it comes to facing (and solving) the global challenges that lie ahead.

1.1. The nitrogen cycle and the role of plants

Nitrogen (N) is an integral part of nucleic acids, proteins and other non-protein compounds, such as co-enzymes or secondary metabolites, which makes it the mineral element required in the greatest amounts by all living organisms. In fact, the availability of N is a major factor limiting plant growth both in natural and agricultural environments, shadowed only by sunlight and water (Greenwood, 1982).

Despite the fact that roughly 78% of the atmosphere is made of molecular nitrogen (N_2), the strong triple covalent bond that characterises this molecule hampers its use by plants, which must therefore find other means to obtain nitrogen. N_2 can, nevertheless, be converted to ammonia (NH_3) through the process of fixation, and later to nitrate (NO_3^-) through nitrification, and thus enter the biological cycles. The means of N_2 fixation include atmospheric fixation (lightning and photochemical conversion to nitrate), the industrial conversion to ammonia (Haber-Bosch process) and biological fixation mediated by bacteria (Kraiser *et al.*, 2011). The latter is catalysed by enzymes called nitrogenases (EC 1.18.6.1 and ED 1.19.6.1) and they are thought to account for the annual production of 65% of fixed nitrogen, a notable contrast to the 25% produced by the Haber-Bosch process (Newton, 2002). NH_3 and NO_3^- can be converted back to N_2 by denitrifying bacteria or they can be assimilated by plants and used in the biosynthesis of organic nitrogen compounds, which then become accessible to other organisms. These are in turn returned to the environment through secretion, excretion or decay of organic matter, and converted back to ammonium by bacteria or fungi (ammonification), in this way closing the nitrogen cycle (Figure 1.1.1).

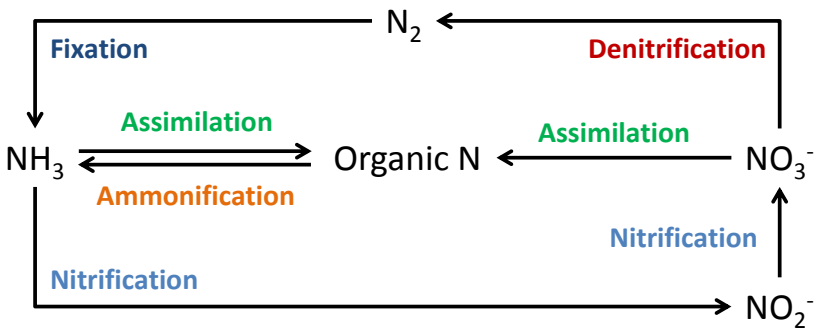

Figure 1.1.1. Schematic and simplified representation of the N cycle. The main inorganic nitrogen species are represented (N_2, NH_3, NO_2^- and NO_3^-) and the processes through which they are converted into each other and into organic N species are indicated.

As mediators of N assimilation, plants play a paramount role in the N cycle, and have therefore evolved systems for the retrieval of both organic and inorganic N from the soil, such as NO_3^-, NH_4^+, urea and amino acids (Marquez *et al.*, 2005; Kraiser *et al.*, 2011). Additionally, some plants can also establish a mutualistic symbiosis with N_2-fixing bacteria, and thus obtain it directly. The most common of this type of symbiosis is the one established between plants of the *Leguminosae* family and the gram-negative bacteria rhizobia. Additionally, symbioses are established between several woody plant species and bacteria of the genera *Frankia*, as well as between cyanobacteria and cycads or ferns, such as the one established between the water fern *Azolla* and *Anabaena* (Taiz and Zeiger, 2002).

As previously mentioned, N is essential for plant growth, which, in a balanced ecosystem is not a limiting nutrient. In agricultural terms, however, the scenario is different, for agriculture is a major disturbance imposed upon the ecosystem. Therefore, global production is determined by N availability, which is mostly supplied in the form of N fertilisers (Newton, 2002). These chemicals, however, are a serious source of pollution and represent the major use of energy in agricultural systems, which ultimately represents a high cost to farmers and society as a whole (Charpentier and Oldroyd, 2010). Also, it is not certain whether the fertiliser industry will cope with the increasing production demands without jeopardising the environment to unsustainable levels, particularly considering the extremely low nitrogen-use efficiency (the amount of N retrieved in food produced per unit of N applied) that characterises their use. In 2005, it was estimated that only 17% of N from N fertilisers applied was consumed by humans in crop, dairy and meat products (Braun, 2007) and the nitrogen-use efficiency of cereals decreased 50% from 1960 to 2000 (Tilman *et al.*, 2002; Beever *et al.*, 2007). This represents vast amounts of fixed N that end up in natural reservoirs, which, besides having negative effects on the environment, such as the unintentional fertilisation of N-limited

ecosystems, causing loss of biodiversity, the decline of the quality of surface and ground waters and an imbalance in the greenhouse gas composition of the atmosphere and the overall air quality, additionally represents an incredible waste of energy during the Haber-Bosch process, with estimated values of 1-2% of the world's total energy supply (Newton, 2002; Smith, 2002; Erisman *et al.*, 2008). In this context, the importance of the symbiosis between legumes and rhizobia is highlighted: the necessity of N fertilisers is abrogated in these plants, diminishing pollution levels and costs for farmers.

In fact, legumes are second only to the Gramineae family, which includes rice, wheat, maize and barley, in terms of agricultural significance and are a major source of organic fertiliser, reason why they are successfully employed in most agricultural rotations (Graham and Vance, 2003). Moreover, their protein-rich composition makes them an important resource both for human nutrition and animal feed (Young *et al.*, 2003).

In conclusion, if farming practises can make use of more economically and ecologically sensible N fixation, with the aim of increasing nitrogen-use efficiency, agriculture, farmers and the environment will benefit, fact that correlates strongly with legumes and their capacity to establish a symbiosis with N_2-fixing rhizobia.

1.2. *Medicago truncatula*: a model system for the study of legume-rhizobia symbiosis

Considering the relevance of the symbiosis established between legumes and rhizobia, an appropriate model plant for the molecular, genetic and systemic study of this relationship was necessary. *Medicago truncatula* (Barrel Medic), a small legume native to the Mediterranean region and with a close relationship with many crop and forage legumes of economic importance, offers many characteristics that enabled it to become such a model, most importantly the fact that it is a diploid plant and has a relatively small genome size (approximately 550 million bp), fact that ultimately facilitates the analysis of scientific problems. Additionally, *M. truncatula* is self-fertile, has a short regeneration period, accounts for an abundant seed production and transformation protocols are well established (Cook, 1999; Trieu *et al.*, 2000).

Apart from its intrinsic characteristics, a vast array of genetic and bioinformatics tools are available for *M. truncatula*. Its genome sequencing project is approaching completion (Cannon *et al.*, 2009) and more than 50.000 genetic probes are offered by Affimetrix®

GeneChip, which covers the majority of genes in this species and allows the development of a gene expression atlas (Benedito *et al.*, 2008; He *et al.*, 2009). Also, a vast library of *Tnt1* mutants exists (Tadege *et al.*, 2008; Tadege *et al.*, 2009), along with an effective protocol for RNA interference (RNAi)-mediated gene silencing (Limpens *et al.*, 2004), powerful reverse genetics tools in the study of gene function.

For the reasons stated above, *M. truncatula* is a useful and adequate model legume for the study of legume-rhizobia interactions. Moreover, the set of experimental tools that are continuously being developed for this model extend its applicability beyond the scope of bacterial symbiosis to other fields of legume biology, which can contribute to research areas such as human nutrition, pathogen and stress responses, root development, hormonal control of plant development, amongst others (Cook, 1999).

1.3. Symbiosis as a means to fix atmospheric nitrogen

M. truncatula and its rhizobial partners, such as *S. meliloti* or *S. medicae*, establish a mutually beneficial endosymbiotic relationship, in which the bacteria provide the plant with the nitrogen it requires and, conversely, the plant supplies the bacteria with carbohydrates and a particular niche for their establishment. This process involves a chain of complex signal exchange, which induces bacterial differentiation and morphological changes in the legume, necessary modifications to the occurrence and maintenance of the symbiotic relationship. The legume first signals the bacteria through the production of flavonoids, aromatic compounds that induce the production of lipochitooligosaccharide compounds by the bacteria through the induction of the *nod* genes (Zuanazzi *et al.*, 1998). These compounds, known as nodulation (Nod) factors, in turn exert several effects on the root of the host plant, which exhibits ion fluxes and expression of Nodulin proteins, eventually becoming infected and undergoing root nodule organogenesis, i.e., the development of the specialized organ where the bacteria convert molecular nitrogen into ammonia (Jones *et al.*, 2007; Oldroyd and Downie, 2008).

In order to achieve a successful symbiosis, root nodule organogenesis must occur at the site of bacterial infection, which means that these events must be spatially and temporally coordinated (Oldroyd and Downie, 2004). These are dependent upon the plant's recognition of the rhizobial lipochitooligosaccharide Nod factor (NF), which, despite being produced by the bacteria, can be said to behave similarly to plant hormones, for NFs are diffusible signals responsible for the activation of diverse developmental processes in the plant (Oldroyd and

Downie, 2008). Considering the low concentrations at which Nod factors are active, which can be as low as 10^{-12} M, inducing nodule formation exclusively in host plants, the hypothesis of a high-affinity NF receptor on the host has long been formulated (Heidstra and Bisseling, 1996). However, up until now, the mechanism of NF recognition has not been fully described.

Numerous responses are induced in the host plant when in contact with Nod factors. An increase in the intracellular levels of Ca^{2+} in root hairs is seen, followed by Ca^{2+} spiking (Oldroyd and Downie, 2004). Also, the production of a nonflavonoid compound occurs, which causes a further increase in the induction of the *nod* genes (van Brussel *et al.*, 1990), as well as the expression of chalcone synthase, a key enzyme in the biosynthesis of flavonoids (Yang *et al.*, 1992). Moreover, expression of chitinases that degrade Nod factors, thus controlling their concentration or selectively destroying nonspecific factors, is verified (Staehelin *et al.*, 1994; Ovtsyna *et al.*, 2000) and there are changes in the plant's hormone balance (Hirsch and Fang, 1994; Mathesius *et al.*, 2000), along with the increased production of reactive oxygen species (Baier *et al.*, 1999). These responses to Nod factors are required for the formation of infection threads, which are specialised transcellular apoplastic compartments filled with bacteria that penetrate into the plant cortical tissue and deliver the bacteria to their target cells (Fournier *et al.*, 2008). Plant cells in the inner cortex engulf the invading bacteria in host-membrane-bound compartments that mature into structures known as symbiosomes. The internalised bacteria then differentiate into bacteroids and are capable of N_2 fixation (Figure 1.3.1).

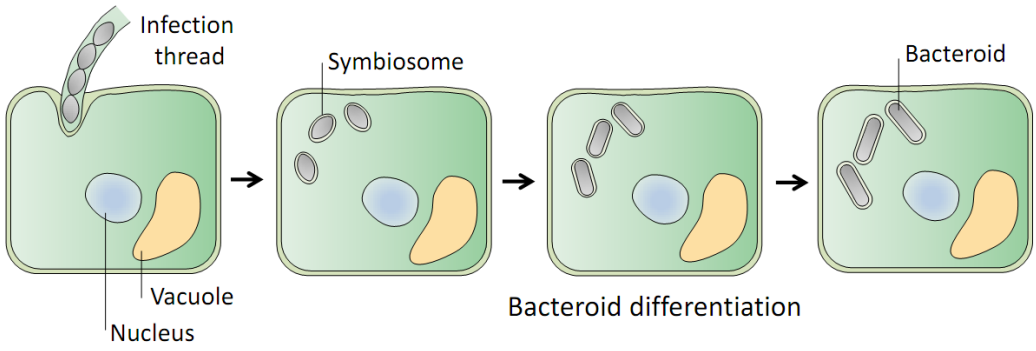

Figure 1.3.1. Endocytosis of bacteria in infection threads and bacteroid differentiation.

Legumes establish two distinct types of nodules: indeterminate nodules, such as the ones formed by *M. truncatula* and other temperate legumes, and determinate nodules, as happens in tropical legumes, such as *L. japonicus* (Patriarca *et al.*, 2004). These different types of nodules have distinct anatomies and while indeterminate nodules have an elongated shape divided into five specific zones, determinate nodules are spherical in shape. In mature nodules

of *M. truncatula*, peripheral uninfected tissues surround central infected cells and the complex yet highly organized anatomy in which they are assembled is essential for nodule function. The bacterial nitrogenase is irreversibly inhibited by O_2 and even the transcription of the genes required for fixation occurs only in conditions of low oxygen pressure. Its activity, however, requires high amounts of ATP (adenosine triphosphate), which can only be supplied by aerobic respiration. Nodule structure provides the required oxygen barrier (Minchin, 1997) and the expression of leghæmoglobin, a high-affinity O_2-carrier protein, allows release of O_2 to the bacteroids (Ott *et al.*, 2005), which then act as an O_2 sink by using a cytochrome oxidase with high-affinity for oxygen (Preisig *et al.*, 1996). In this way, the flux of O_2 is tightly controlled and N_2 fixation can occur.

When root nodule development is complete, a functional symbiosis is established, characterized by reciprocal metabolic exchanges. Amongst these are transport of NH_3/NH_4^+ from the bacteroid, where it is produced, to the plant cytosol, where it is assimilated into glutamine, and transport of dicarboxylic acids originating in the plant to the endosymbiotic bacteroid. Other metabolites are provided to the bacteroid by the plant host, namely branched-chain amino acids (Prell *et al.*, 2009) and homocitrate (Hakoyama *et al.*, 2009). This nutrient exchange requires transport across both the bacteroid and the symbiosome membrane, and the molecular identity of some transporters remains to be identified, including that of the symbiosome NH_4^+ transporter.

1.4. The fundamentals of N metabolism in *Medicago truncatula*

Irrespective of the primary N source, prior to assimilation into an organic form, inorganic N is always converted to NH_4^+ (Lam *et al.*, 1996), which is then assimilated into glutamine (Gln) and glutamate (Glu). Glutamine synthase (GS) is the first and one of the main enzymes involved in this pathway of nitrogen assimilation, along with glutamine-2-oxoglutarate aminotransferase (GOGAT). Besides primary assimilation, these enzymes play distinct and coordinated roles in the reassimilation of ammonia originating from photorespiration and in the recycling of nitrogen derived from protein degradation, amino acid catabolism and specific metabolic pathways, such as the metabolism of phenylpropanoid (Lam *et al.*, 1996; Schjoerring *et al.*, 2002)(Figure 1.4.1). GS (E.C. 6.3.1.2) is responsible for the ATP-dependent condensation NH_4^+ of with Glu to yield Gln (Bernard and Habash, 2009). In turn, the enzyme GOGAT (EC 1.4.7.1 and EC 1.4.1.14) catalyses the transfer of the amide group of Gln to

2-oxoglutarate, producing two molecules of Glu, which can serve as substrate for the GS reaction or for the aminotransferase-mediated synthesis of amino acids (Forde and Lea, 2007; Lea and Miflin, 2010) (Figure 1.4.1).

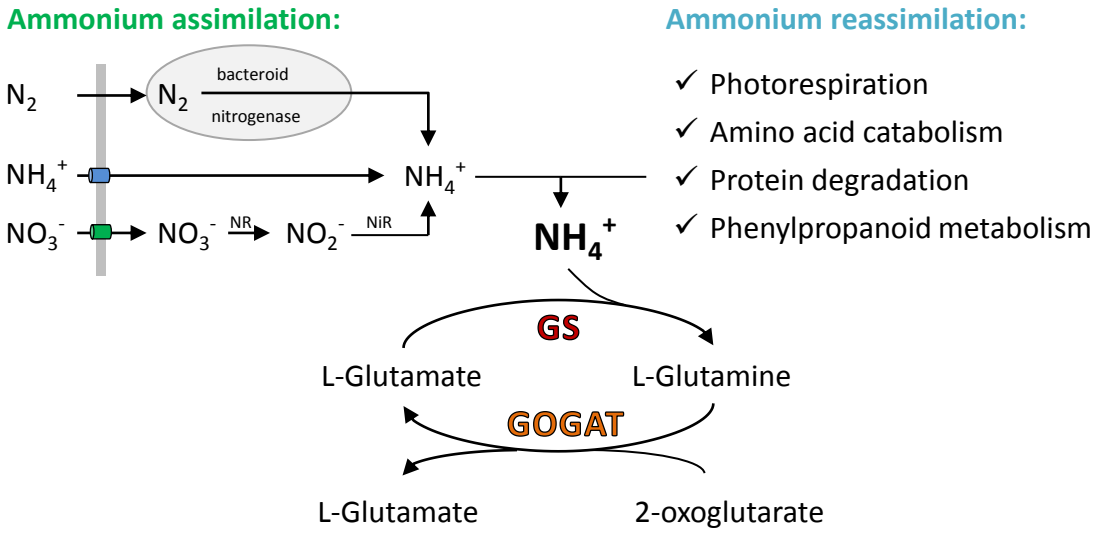

Figure 1.4.1. The process of nitrogen assimilation and reassimilation in plants. Nitrogen originating in primary sources (N_2, NH_4^+, and NO_3^-) and secondary sources is converted to NH_4^+ and incorporated into glutamate, yielding glutamine, a reaction catalysed by glutamine synthetase (GS). Glutamine and 2-oxoglutarate originate two molecules of glutamate via the enzyme glutamine-2-oxoglutarate aminotransferase (GOGAT). NR – Nitrate reductase; NiR – Nitrite reductase.

1.4.1. Glutamine synthetase

In *M. truncatula*, the GS gene family is composed of four expressed genes: two cytosolic isoforms (*MtGS1a* and *MtGS1b*) and two plastidial isoforms (*MtGS2a* and *MtGS2b*). A third cytosolic GS exists, which is not expressed (*MtGS1c*) (Stanford *et al.*, 1993; Carvalho *et al.*, 1997; Melo *et al.*, 2003; Seabra *et al.*, 2010). The pattern of expression of each GS gene is distinct and they appear to participate in different metabolic processes, which accounts for a tight regulation of their expression and activity. Overall, cytosolic GS1 isoenzymes are involved in N assimilation and recycling originating from numerous physiological processes (Bernard and Habash, 2009), while the role of the plastidial GS2 has been mainly associated with the reassimilation of the ammonia released during photorespiration (Wallsgrove *et al.*, 1987; Orea *et al.*, 2002). In *M. truncatula*, *MtGS1a* is significantly upregulated in root nodules, where it accounts for more than 90% of total GS activity, and this isoenzyme is therefore the main

responsible for the assimilation of ammonia originating from N_2 fixation (Stanford *et al.*, 1993; Carvalho *et al.*, 1997). *MtGS1b* is significantly upregulated in roots, which correlates with a N assimilation function (Stanford *et al.*, 1993) and *MtGS2a* is highly expressed in photosynthetic tissues, where it is the isoenzyme that contributes the most for total GS activity, which correlates with the reassimilation of the ammonia released during photorespiration (Carvalho *et al.*, 1997; Melo *et al.*, 2003). *MtGS2b*, on the other hand, is expressed exclusively in developing seeds and its function was associated with the accumulation of storage protein (Seabra *et al.*, 2010).

At the posttranscriptional level, the *MtGS* genes have been shown to be regulated in different manners. *MtGS2a* is phosphorylated by Ca^{2+}-dependent kinase(s) and this phosphorylation allows interaction with 14-3-3 proteins, which then leads to selective proteolysis of the plastid located isoform, resulting in inactivation of the isoenzyme (Lima *et al.*, 2006). *MtGS1a* and *MtGS1b* are also targets for phosphorylation, yet by a Ca^{2+}-independent kinase. This posttranslational modification is affected by light in leaves and by active N fixation in root nodules, which suggests a connection of this mechanism with nodule functioning (Lima *et al.*, 2006).

MtGS1a is also a target for nitric oxide (NO) and suffers NO-mediated inactivation through tyrosine nitration. An increase in nodule GS nitration occurred in conditions in which nitrogen fixation is impaired and GS activity reduced (ineffective (Fix^-) and NO_3^--treated nodules) and it was suggested that this posttranslational inactivation was related to metabolite channelling, in order to boost the nodule antioxidant defences in response to NO (Melo *et al.*, 2011).

1.4.1.1. Regulation of GS expression by inorganic nitrogen

The application of external inorganic nitrogen has been shown to modulate GS expression, but the extent, significance and result of this control varies between plant species, the N source and the plant organ/tissue, in a way that makes it difficult to ascribe a definite regulatory role to a given N source, especially considering the diversity of experimental set-ups described in the literature. In soybean (*Glicine max*), nitrate treatment did not affect expression of two GS1 genes, yet external supply of ammonium led to the upregulation of these genes (Hirel *et al.*, 1987). In *Arabidopsis thaliana*, ammonium treatment caused different responses in each of the GS1 genes, leading to increased levels of *AtGln1;2* and decreased levels of *AtGln1;1*, whereas the levels of *AtGln1;3* remained unaffected (Ishiyama *et al.*, 2004). In radish (*Raphanus sativus*) and maize (*Zea mays*), differential responses were also seen

between cytosolic GS genes after treatment with inorganic N. In the first case, increased expression of *RsGln1;1* and decreased expression of *RsGln1;3* were observed (Watanabe *et al.*, 1994). In the latter, increased levels of *ZmGS1;1* were seen, yet the variation of *ZmGS1;2* in response to inorganic N varied between shoots and roots, given that upregulation was observed in the former and downregulation in the latter. This type of tissue specific variations in response to external N were also reported in rice (*Oryza sativa*), as in surface cell layers of roots *OsGln1;1* is upregulated under N-limiting conditions and *OsGln1;2* is upregulated under N-sufficient conditions, variations that are not detected in the central cylinder of roots (Ishiyama *et al.*, 2004). These are but a few examples that illustrate the complexity of this control, especially considering that the GS family is a multigene one.

In the *Medicago* genus, a couple of studies tried to describe this relationship, but until this moment it is still not clear. Stanford *et al*. (1993) saw no significant variations of the expression of *MtGS1a* and *MtGS1b* under different N regimes, with only minor increases of the expression of both genes in response to 2 mM NO_3^- and of *MtGS1b* in response to 2 mM NH_4^+. In these experiments, plants were continuously grown with each N source and thus a specific response to a change in the environmental conditions cannot be deduced from these data. These authors also performed starvation and readdition experiments, but saw no variations in the levels of *MtGS1a* and *MtGS1b* under up to six days of starvation, nor did they after the readdition of NH_4^+. Readdition of NO_3^- showed only a slight increase after 24 hours, a value that returned to normal within three days. They conclude by stating that N supply is not the key effector in the regulation of GS genes in *M. truncatula*, but that it still has some effect. Recently, a study showed an increase in the protein amounts of GS1 and GS2 in roots, following a two-day treatment with 10 mM NH_4NO_3 (Melo *et al.*, 2011). Studies performed in *M. sativa* aimed at describing specific responses to changes in the environmental N status, thus seedlings were grown under N starvation for three weeks and analysed after 1.5 days of treatment with NO_3^- and NH_4^+. Nitrate led to upregulation of *MsGS2* in leaves and roots, but no significant differences were detected in protein abundance. Ammonium treatment did not affect the expression of *MsGS2*. These authors also found that the response to NO_3^- peaked at 1.5 hours of treatment in roots, but this maximum was delayed in leaves. In these organs, significant increases in *MsGS2* were seen after 2 hours and started to decrease after 6, returning to initial values after 36 hours (Zozaya-Hinchliffe *et al.*, 2005). This shows that specific modulatory mechanisms affect GS in response to the external administration of inorganic N, probably occurring at the transcriptional and posttranscriptional levels. The precise nature of this control, however, is not yet clear.

1.4.2. Discriminating potential sensors and regulators

A conceivable way to identify sensors and regulators in a given metabolic pathway is to compromise the function of key players in that same pathway and look for significant differences. Given the central position that GS occupies in the metabolism of nitrogen, it comprises an ideal target for the identification of new and important players in the metabolic network.

Recently, a transcriptomic analysis of symbiotic nodules impaired in N assimilation through the inhibition of GS with phosphinothricin (PPT) identified several genes that could function as N sensors and/or regulators (Seabra *et al.*, 2012). Noteworthy was the downregulation of a transcript annotated as ammonium transporter 3 (*MtAMT3*) and the upregulation of both a putative nitrate reductase (*MtNR3*) and a putative transcription factor, *NIN*-like protein 7 (*MtNLP7*) (Seabra *et al.*, 2012). Additional evidence suggests an involvement of these genes as regulators of N metabolism, as detailed in the following paragraphs.

1.4.2.1. Ammonium transporter 3

Ammonium transport into roots has biphasic kinetic properties in several species (Fried *et al.*, 1965; Vale *et al.*, 1988; Wang *et al.*, 1993). The high-affinity ammonium transport system (HATS) is predominant at submillimolar external ammonium concentrations and saturates as the concentration increases. In this system, the driving force for the ammonium uptake is the membrane electric potential and NH_4^+ is its substrate. Conversely, the low-affinity ammonium transport system (LATS) is significant at higher external ammonium concentrations (>1 mM) and does not saturate with increasing concentrations of ammonium (Walker *et al.*, 1979; Ullrich *et al.*, 1984; Ayling, 1993; Wang *et al.*, 1993; Kronzucker *et al.*, 1996). The latter has not been as well characterized as the former and the question remains whether it represents a cation channel with broad specificity, able to transport NH_4^+, or account for the diffusion of NH_3 across the membrane (White, 1996).

The first ammonium transporter described in plants was isolated and cloned from *A. thaliana* in 1994 and is now known as *AtAMT1;1* (Ninnemann *et al.*, 1994). Four more genes have been described since then, composing the AMT1 family of transporters in this model plant. In tomato and rice, similar multigene families have been described (Lauter *et al.*, 1996; Von Wirén *et al.*, 2000). These genes have different expression profiles and biochemical properties, suggesting complementary roles in ammonium uptake in roots and shoots (Gazzarrini *et al.*, 1999; Von Wirén *et al.*, 2000; Shelden *et al.*, 2001). Nevertheless, all

transporters of the AMT1 family are saturable, high-affinity NH_4^+ and methylammonium transporters (Sohlenkamp *et al.*, 2000).

A second group of ammonium transporters, the AMT2 family, was assigned to a separate cluster due to the phylogenetic distance that separated them from the members of the AMT1 family. In fact, these proteins are closer to the Mep1, Mep2 and Mep3 ammonium transporters of *Saccharomyces cerevisiae* and the *Escherichia coli* AmtB transporter than to the AMT1 proteins (Sohlenkamp *et al.*, 2000). In *A. thaliana* and *L. japonicus*, AtAMT2;1 and LjAMT2;1 are also high-affinity NH_4^+ transporters, yet are unable to transport methylammonium. Through protein fusions with GFP (Green Fluorescent Protein), these transporters have been shown to localize to the plasma membrane, providing direct evidence of being transmembrane proteins (Sohlenkamp *et al.*, 2000; Sohlenkamp *et al.*, 2002; Simon-Rosin *et al.*, 2003). In *A. thaliana*, *AtAMT2;1* is more expressed in shoots as opposed to roots and it is upregulated in response to N depletion, but only in roots (Sohlenkamp *et al.*, 2000; Sohlenkamp *et al.*, 2002). In *L. japonicus*, *LjAMT2;1* is expressed in both infected and uninfected tissues of the nodule and these observations suggested that this transporter might play a role in the recovery of ammonium that is lost from nodule cells to the apoplast. Additionally, in both model species, AMT2;1 could be involved with the recovery of ammonium lost from plant cells during normal metabolism in other organs, such as shoots and leaves, where it is highly expressed (Simon-Rosin *et al.*, 2003).

In the legume-rhizobia symbiosis, the current model of NH_3 transport from the bacteroid to the plant cytosol devises a passive transport of NH_3 to the peribacteriod space, where it is protonated given its lower pH, an acid-trap that guarantees a concentration gradient, followed by active transport of NH_4^+ across the symbiosome membrane to the plant cytosol (Tyerman *et al.*, 1995; Day *et al.*, 2001). However, in *M. truncatula*, functional studies on ammonium transporters have not yet been performed and, most importantly, the molecular identity of the ammonium transporter in the symbiosome membrane has not been revealed. In this context, the sustained PPT-induced downregulation of *MtAMT3* makes this an interesting gene to explore in terms of the subcellular localization and functionality of the protein it encodes.

1.4.2.2. Nitrate reductase 3

Nitrate reductase (NR) is a key enzyme for N assimilation in plants that reduces nitrate to nitrite by an NAD(P)H-dependent mechanism, an essential step before its further reduction to NH_4^+, substrate for GS. However, several lines of evidence have shown that in plants nitrate reductase is responsible for the evolution of NO_x species, in particular, nitric oxide, using nitrite

and NADH as substrates (Dean and Harper, 1988; Yamasaki *et al.*, 1999; Rockel *et al.*, 2002). This nitrite-reducing activity of NR has been supported by the observation that NO emission is reduced in NR-deficient organisms, such as *Chlamydomonas* (Sakihama *et al.*, 2002), *N. benthamiana* (Yamamoto-Katou *et al.*, 2006) or *A. thaliana* (Shi and Li, 2008). The NO-evolution function of NR is highly relevant considering that NO is now widely recognized as an endogenous signalling molecule involved in physiological processes that extend from plant growth and development (del Río *et al.*, 2004; Delledonne, 2005) to stress responses (Wendehenne *et al.*, 2001; Gould *et al.*, 2003), and the legume-rhizobia symbiosis is no exception. NO production has been detected in *L. japonicus* and *M. sativa* roots after infection with *Mesorhizobium loti* and *S. meliloti*, respectively (Shimoda *et al.*, 2005; Nagata *et al.*, 2008). In *M. truncatula*, it was recently shown that NO is required for the establishment of symbiosis and its production was detected during growth of infection threads and in nodule primordia (del Giudice *et al.*, 2011), yet it was restricted to the fixing zone of the nodule (Baudouin *et al.*, 2006). In plants infected with an auxin-overproducing strain of rhizobium, which show increased nodulation, higher levels of NO were measured (Pii *et al.*, 2007). Yet the positive way through which NO affects nodule formation is counterbalanced by the negative effect it exerts in fixation. Besides inhibiting the bacterial nitrogenase directly (Trinchant and Rigaud, 1982), NO binds readily with leghæmoglobin (Meakin *et al.*, 2007), competing with oxygen, and thus causing O_2-mediated inhibition of nitrogenase. The overall result is a decrease in nitrogenase activity and nitrogen fixation (Trinchant and Rigaud, 1982; Kato *et al.*, 2010). In fact, when a NO donor is applied, a decrease in fixation is seen, and the opposite effect is observed with the addition of a NO scavenger (Shimoda *et al.*, 2009; Kato *et al.*, 2010). Accordingly, when *M. truncatula* is infected with a rhizobium strain mutant for the flavohæmoglobin Hmp, a NO-degrading enzyme, a decrease in N fixation is visible (Meilhoc *et al.*, 2010). Finally, a wide range of genes has been shown to respond to NO during the establishment of a functioning nodule, which points to a possible contribution of NO in nodule metabolism (Ferrarini *et al.*, 2008), including glutamine synthetase (Melo *et al.*, 2011).

Simultaneously, the source of NO in nodules has not yet been fully elucidated, but in the context of the symbiosis it can originate either in the plant, the bacteria or both. In the bacteria, the denitrification pathway was recently shown to be the main source of NO in *Bradyrhizobium japonicum-Glycine max* symbiotic nodules in response to flooding (Zumft, 1997; Sánchez *et al.*, 2010). From the plant's perspective, NO synthase (NOS)-like proteins have been proposed as a NO source, given that NOS-like activity has been seen in different systems (Cueto *et al.*, 1996; Baudouin *et al.*, 2006). Nevertheless, to this date, only the sequences of two plant NOS enzymes have been described, which belong to two green algal

species of the genus *Ostreococcus* (Foresi *et al.*, 2010). As mentioned previously, NR can also yield NO in the presence of nitrite and NADH and it was recently shown in *M. truncatula* that both plant and bacterial NRs are involved in NO synthesis. Moreover, a nitrate-NO respiration process with the purpose of maintaining the energy status under oxygen-limiting conditions was proposed (Horchani *et al.*, 2011). This poses a new role for NR in the context of nodule metabolism, which is still not fully elucidated, further enticed by the upregulation of *MtNR3* observed in response to PPT-mediated inhibition of GS in nodules.

1.4.2.3. NIN-like protein 7

NIN (Nodule inception) proteins are essential in nodule development in legumes (Schauser *et al.*, 1999; Marsh *et al.*, 2007), but NIN-like genes are also found in non-legume plants and algae.

Recently, it was shown that the *MtNLP7* homologue in *A. thaliana*, *AtNLP7*, is a transcription factor regulating N assimilation (Castaings et al., 2009). *Atnlp7* mutants show a phenotype characteristic of N-starved plants and are impaired in transduction of the nitrate signal, as they fail to completely induce nitrate-responsive genes after a short N starvation period followed by nitrate re-supply (the high-affinity nitrate transporters *AtNRT2;1* and *AtNRT2;2*, as well as nitrate reductase-encoding genes *AtNIA1* and *AtNIA2*). This study also showed that *AtNLP7* is targeted to the nucleus, which supports the hypothesis of *NLP7* acting as a transcription factor (Castaings *et al.*, 2009). Previously, the *Chlamydomonas reinhardtii NIT2* gene, an orthologue to *AtNLP7* and *MtNLP7*, had also been proposed as a transcription factor mediating N status (Camargo et al., 2007). The Nit2 protein binds the *CrNIA1* promoter and activates its expression, in the presence of intracellular NO_3^-. Additionally, the expression of *CrNIT2* is negatively controlled by ammonium and optimum in N-free medium (Camargo *et al.*, 2007). Moreover, it was show that *CrNIT2* has a negative effect in the expression of the putative ammonium transporter *CrAMT1* (Gonzalez-Ballester *et al.*, 2004), which correlates well with the negative effect that ammonium has over *CrNIT2* expression. This dual-role connects the ammonium uptake and the nitrate assimilation pathways, placing Nit2 in a central position in the metabolism of nitrogen in this system.

1.5. Thesis outline

In the context of the legume-rhizobium symbiotic interaction, this thesis is dedicated to the study of the metabolism of nitrogen from the plant's perspective. Using *Medicago truncatula* and *Sinorhizobium meliloti* and *Sinorhizobium medicae* as a model system for the legume-rhizobia symbiosis, the potential of putative N sensors and regulators of N metabolism and the response of central genes in this metabolic network to environmental cues began to be evaluated. In particular, this thesis aimed at providing an initial description of the function of *MtAMT3*, *MtNR3* and *MtNLP7* in the legume-rhizobium symbiosis, both by resorting to the available bioinformatics tools and through their response to different N environments. Additionally, and considering its central role in N metabolism, this thesis intended to verify whether there is a direct response of GS to N-supply after N-starvation.

The experimental work performed is presented in the following chapters, including the materials and methods employed (Chapter II), the main results obtained (Chapter III) and their discussion (Chapter IV). Initially, the sequences of *MtAMT3*, *MtNR3* and *MtNLP7* were subjected to a bioinformatic analysis with the aid of the available databases and studied according to the existing information regarding their homologues. Subsequently, the expression of these genes in nodules grown under different N conditions was assayed, so that possible clues regarding their function in these environments could be obtained. For *MtNLP7*, this analysis was deepened and an RNA interference strategy for the study of gene function was initiated. Finally, the expression of these genes and those of GS was evaluated in three-week old seedlings upon the treatment with different N sources, under distinct concentrations and at two time points, with the purpose of finding specific responses to environmental cues.

Lastly, this thesis ends with the summary of the main conclusions derived from this work and with the identification of future challenges, key questions and ideas for future research (Chapters V and VI).

Chapter II

Materials and Methods

2.1. Biological material

2.1.1. Plant material and growth conditions

Plants of *M. truncatula* Gaertn. cv Jemalong were grown in aeroponic conditions under 16 h light (20 ^{0}C)/8 h dark (19 ^{0}C) cycles under a light intensity of 150 to 200 µmol·m^{-2}·s^{-1} in growth medium supplemented with NH_4NO_3 as described by Lullien *et al.* (1987). For nodule induction, plants were nitrogen starved for four days before inoculation with either the *Sinorhizobium meliloti* effective wild-type strain, the *Sinorhizobium medicae* effective wild-type strain or the ineffective *fixJ* (Fix$^-$) *S. meliloti* mutant (GMI 347). Nodules were harvested 20 days post infection (dpi). For the experiment with nitrate, nodulated plants (20-dpi) were aeroponically grown for 2 days in growth medium containing 10 mM KNO_3 before harvesting.

For the studies on the effect of N nutrition in three-week old seedlings, seeds of *M. truncatula* Gaertn. cv Jemalong were treated with H_2SO_4 for 10 minutes, washed with water, sterilized in bleach for 10 minutes and washed with sterile water three times in the laminar flow chamber. Subsequently, seeds were spread on agar plates and incubated at 18 ^{0}C in the dark for 24 hours. The plates were then exposed to light and grown for three weeks under 16 h light (20 ^{0}C)/8 h dark (19 ^{0}C) cycles under a light intensity of 200 µmol·m^{-2}·s^{-1}. At the end of this period, seedlings were randomly divided amongst plates containing different solutions imbibed in filter paper (phosphate buffer control and 0.5 mM KNO_3, 10 mM KNO_3, 0.5 mM $NH_4H_2PO_4$ or 10 mM $NH_4H_2PO_4$ in phosphate buffer). Seedlings were incubated in these conditions for 3 or 24 hours, time at which they were pooled in groups of three or four, had their root and aerial part separated with a scalpel and were flash frozen in liquid nitrogen.

For *Agrobacterium rhizogenes*-mediated transformation, seeds were germinated as described above, with the exception that incubation occurred upside-down and only for 30 hours, time at which the transformation was performed (as described in Chapter 2.8). After

the transformation with *A. rhizogenes* and following 20 days of growth in agar plates, transformed plants were grown aeroponically. For nodule induction, plants were nitrogen starved for four days before inoculation with *S. medicae*.

All plant material was immediately frozen in liquid nitrogen and stored at -80 ^{0}C.

2.1.2. Bacterial strains and plasmids used

The bacterial strains and plasmids used are listed in Table 2.1.1.

Table 2.1.1. List of bacterial strains and plasmids used

Bacterial strains or plasmids	Pertinent features	Origin or reference
Escherichia coli		
DH5α	*supE*44 Δ*lac*U169 (Φ80 *lacZ*ΔM15) *hsdR*17 *recA*1 *endA*1 *gyrA*96 *thi-1 relA*1	(Irwin and Janssen, 2001)
Sinorhizobium spp.		
S. meliloti GMI 151	Wild-type strain	(Rome *et al.*, 1996)
S. medicae		(Rome *et al.*, 1996)
S. meliloti GMI 347	Mutant (*fixJ*) strain, unable to fix atmospheric N_2.	
Agrobacterium rhizogenes		
Plasmids		
pCRblunt	*lac*Zα-*ccd*B fusion under the *Lac* promoter	Invitrogen™
pRNAi	Double CaMV 35S promoter and OCS terminator separated by a 335 bp spacer with restriction sites flanking both promoter and terminator	(Limpens *et al.*, 2004)
pGreen 0029	Binary vector with a nos-kan cassette inserted into the *Hpa*I site of the Left Border, providing resistance to kanamycin	(Hellens *et al.*, 2000)
pSoup	Helper plasmid, provides replication functions in *trans* for pGreen in *Agrobacterium*	(Hellens *et al.*, 2000)
pRNAi-Down	pRNAi-derivative containing the NLP7 insert upstream the OCS terminator in sense orientation	This work
pRNAi-Up-Down	pRNAi-Down-derivative containing the NLP7 insert downstream the d35S promoter in the antisense orientation	This work
pGreen-RNAi-NLP7	pGreen-derivative with the RNAi-NLP7 insert interrupting the *lac*Z gene	This work

2.2. Oligonucleotide sequences used

Oligonucleotide sequences used in PCR reactions are listed in Table 2.2.1.

Table 2.2.1. List of oligonucleotide sequences used (5´- 3´) (n. a. – Not applicable)

Name	Sense	Antisense	Amplicon
Elf1α	CCACCAACCTTGACTGGTAC	CCACGCTTGAGATCCTTCAC	319 bp
AmT	CTGGTGGTTATGTTATTCATC	CAATGTTGGCAGAGTAGG	192 bp
NRx	ATGGGATCTGGCTAATAACACG	TTTGAGGCTTGTGCATGTTTG	107 bp
NLP7	ACATGGACGATGATAATGAATGG	AACTTAACTATGTACGGACACTTG	185 bp
GS1a	GTGTTCTTCTTCTTCCTTCAC	GGTGTAAACATCACAAATCAC	320 bp
GS1b	ATAAGCCACCACGCTACTTC A	AACCATAACAAGGACTCAGATC	168 bp
GS2a	TCATTGAACCCATTTCCTAAG	CCAGAGTTGACTGCCATTAC	295 bp
M13	CAGGAAACAGCTATGACC	TGTAAAACGACGGCCAGT	n. a.

2.3. Plasmid DNA extraction

Plasmid DNA was either extracted using the ZR Plasmid Miniprep™-*Classic* according to the instructions of the manufacturer (Zymo Research Corp.) or following the alkaline method, described in the next paragraph.

Three to five mL of an overnight culture were centrifuged for 1 minute at 13000 rpm and the supernatant was discarded. The pellet was resuspended in 100 µL of Solution I (50 mM glucose; 25 mM Tris; 10 mM EDTA; 100 $\mu g \cdot mL^{-1}$ RNase; pH 8.0) and vortexed, followed by the addition of 200 µL of fresh Solution II (0.2 M NaOH; 1% SDS). The tube was inverted several times prior to an incubation of five minutes on ice. 150 µL of Solution III were added (5 M KCH_3COO; glacial CH_3COOH to a final concentration of 11.5%; pH 4.8), the tube was inverted several times and incubated on ice for five minutes. This was followed by a 5-minute centrifugation (13000 rpm), which allowed the separation of the precipitated proteins and other cellular debris and the plasmid DNA. 360 µL of the supernatant were removed, 100 µL of 100% ethanol were added and the mixture was incubated at -80 ^{0}C for at least 30 minutes, allowing DNA precipitation, which was followed by centrifugation (five minutes; 13000 rpm). The pellet was washed with 70% ethanol and centrifuged again for five minutes (13000 rpm). Finally, the pellet was left to dry and resuspended in 20 µL of water.

2.4. RNA extraction and cDNA synthesis

For the studies of the expression of *MtAMT3*, *MtNR3* and *MtNLP7* in nodules, total RNA was extracted from 100 mg of plant material using the RNeasy® Plant Mini Kit (QIAGEN) according to the instructions of the manufacturer. A subsequent step of on-column DNase digestion was included. Concentration and purity was determined by spectrophotometry and integrity was confirmed by gel electrophoresis (7% formaldehyde, 1% (w/v) agarose (USB®,USA), RNase-free). The ratio of the absorbance at 260 and 280 nm ($A_{260/280}$) was approximately 2.14 in all samples, which is an indicative of sample purity. Sample Fix^- and its respective control were subject to total RNA precipitation in order to increase the RNA concentration in sample Fix^-. RNase-free water was added to a total volume of 100 µL to each sample, following the addition of 50 µL of 7.5 M RNase-free NH_4OAc, 0.5 µL of 5 $mg \cdot mL^{-1}$ RNase-free glycogen and 250 µL of 100% ethanol. RNA precipitated overnight at -20 ^0C, was centrifuged for 30 minutes (12000 g, 4 ^0C) and the pellet was washed twice with 500 µL of 80% ethanol followed by a centrifugation for 5 minutes (12000 g, 4 ^0C). The pellet was left to dry and resuspended in 10 µL of RNase-free water. The $A_{260/280}$ values were 1.88 and 1.97, for control and Fix^- samples, respectively. cDNA was obtained from 1.290 µg of RNA sample using the NZY Reverse Trancriptase (nzytech) according to the instructions of the manufacturer.

For the studies on the effect of N nutrition in three-week old seedlings, total RNA was extracted from 100 mg of plant material using the InviTrap® Spin Plant RNA Mini Kit (STRATEC Molecular) according to the instructions of the manufacturer. A subsequent step of on-column DNase digestion was included. Concentration and purity was determined by spectrophotometry and integrity was confirmed by gel electrophoresis (7% formaldehyde, 1% (w/v) agarose (USB®,USA), RNase-free). The ratio of the absorbance at 260 and 280 nm ($A_{260/280}$) was approximately 2.18 in all samples, which is an indicative of sample purity. cDNA was obtained from 360 to 1102.5 ng of RNA sample (depending on the initial RNA concentration and the desired final concentration of each sample) using the NZY Reverse Trancriptase (nzytech) according to the instructions of the manufacturer.

2.5. Standard and quantitative real time PCR

For each primer pair and each sample tested, polymerase chain reaction (PCR) was performed using 1.25 units of *Taq* DNA Polymerase (Sigma-Aldrich® and Fermentas) in 25 µL

reactions (30 ng of cDNA as template, 0.2 mM dNTP's, 0.2 µM primers, 1.5 or 3 mM MgCl). The conditions of the PCR were the following: initial denaturation (3 min at 95 ^{0}C), followed by 30 or 35 cycles of amplification (15 seconds at 95 ^{0}C; 30 seconds at the primers annealing temperature and 30 seconds at 72 ^{0}C) and a final extension of 5 minutes at 72 ^{0}C. The products of PCR reactions were resolved in 0.8% or 2% (w/v) agarose gels (SeaKem® LE Agarose, Cambrex, USA) 1 µg.mL^{-1} ethidium bromide in TAE Tris-Acetate-EDTA buffer, along with a 1 kb DNA ladder (1 Kb Plus DNA Ladder, Invitrogen™, USA). Band intensity and normalisation was achieved using the TotalLab Quant® software.

Quantitative real-time PCR (qPCR) was performed using an iCycler Thermal Cycler (BIO-RAD) detection system with iQ™ SYBR® Green Supermix (BIO-RAD). Prior to sample analysis, a calibration curve was constructed for each primer set, using two technical replicates per data point and six data points corresponding to 0, 10, 25, 50, 75 and 100 ng of cDNA, in 20 µL of reaction mix, including 250 nM of each primer. This allowed the determination of the amplification efficiency (E) for each primer set, which is given by the slope of the trend line established between the amount of template DNA and the quantification cycle (C_q). These values were found to be 67%, 80%, 134% and 115% for *Mtelf1α*, *MtAMT3*, *MtNR3* and *MtNLP7*, respectively. Samples were measured in technical duplicates using 50 ng of cDNA.

The conditions of the qPCR were the following: initial denaturation (3 min at 95 ^{0}C), followed by 40 cycles of amplification and quantification (10 seconds at 95 ^{0}C; 30 seconds at 55 ^{0}C and 30 seconds at 72 ^{0}C, with a single fluorescence measurement). A melt curve was also generated to verify the specificity of the amplification reaction (55 ^{0}C to 95 ^{0}C, with a fluorescence measurement every 0.5 ^{0}C).

Calculation of C_q was performed by the iQ™ 5 Optical System Software (Version 2.1). The calculation of the relative expression ratio was performed using the mathematical model described by Pfaffl (2001) and summarized in the following equation, where *target* refers to the gene being evaluated.

$$Relative\ Expression\ Ratio = \frac{E_{\text{target}}{}^{C_{q,\text{target,control}} - C_{q,\text{target,test}}}}{E_{elf1\alpha}{}^{C_{q,elf1\alpha,\text{control}} - C_{q,elf1\alpha,\text{test}}}}$$

The qPCR products were resolved in a 0.8% (w/v) agarose gel (SeaKem® LE Agarose, Cambrex, USA) 1 µg.mL^{-1} ethidium bromide in TAE Tris-Acetate-EDTA buffer, along with a 1 kb DNA ladder (1 Kb Plus DNA Ladder, Invitrogen™, USA).

2.6. Protein extraction, determination of GS activity and western immunoblotting

The root and aerial parts of three-week old seedlings of *M. truncatula* were homogenized at 4 ^{0}C in 200 µL of extraction buffer (10 mM Tris; 5 mM L-glutamate sodium salt; 10 mM $MgSO_4 \cdot 7H_2O$; 1 mM dithiothreitol; 0,05% Triton X-100) with insoluble polyvinylpyrrolidone and the homogenates were centrifuged at 20000 g for 20 min at 4 ^{0}C.

GS transferase activity was determined as described by Cullimore and Sims (1980). Briefly, 50 µL of crude extract were incubated in a water bath at 30 ^{0}C in a 1 mL reaction (80 mM Tris-base; 100 mM L-glutamine; 60 mM hydroxylamine hydrochloride; 1.0 mM $MnCl_2 \cdot 4H_2O$; 0.05 mM adenosine 5'-diphosphate sodium salt; 20.5 mM $NaHAsO_4 \cdot 7H_2O$). The reaction was stopped after 30 minutes through the addition of 1 mL of a mixture of 26 $g \cdot L^{-1}$ $FeCl_3$, 40 $g \cdot L^{-1}$ trichloroacetic acid in 9% (V/V) HCl. One unit of transferase activity is equivalent to 1 $\mu mol \cdot min^{-1}$ γ-glutamyl hydroxamate produced at 30 ^{0}C. Activity data were expressed as means plus standard deviation of at least two independent experiments, with duplicate technical assays for each sample.

Soluble protein concentration was measured by the method of Bradford (1976) using the Bio-Rad dye reagent (Bio-Rad, Hercules, CA) and bovine serum albumin as a standard.

For western blot analyses, total soluble protein extracts (8.5 µg) were separated by a 18% (w/v) SDS-polyacryamide gel electrophoresis (SDS-PAGE), electroblotted onto nitrocellulose membranes (Whatman® PROTRAN®) and incubated with polyclonal antibody raised against GS overnight (Cullimore and Miflin, 1984). Immunodetection was performed using goat anti-rabbit horse radish peroxidase conjugated antibody (Santa Cruz Biotechnology) and ECL™ (GE healthcare, Lifesciences) detection system.

2.7. Construction of an RNA interference plasmid for *MtNLP7*

The pGreen-RNAi-NLP7 plasmid contains two perfect inverted repeats of a 185 bp fragment of the coding sequence of *MtNLP7* separated by a 389 bp spacer, with the appropriate promoters and terminators for expression in a plant system and adequate for *Agrobacterium rhizogenes*-mediated transformation. The cloning procedure for the construction of this plasmid is depicted schematically in Figure 2.7.1 and explained in detail in the following paragraphs.

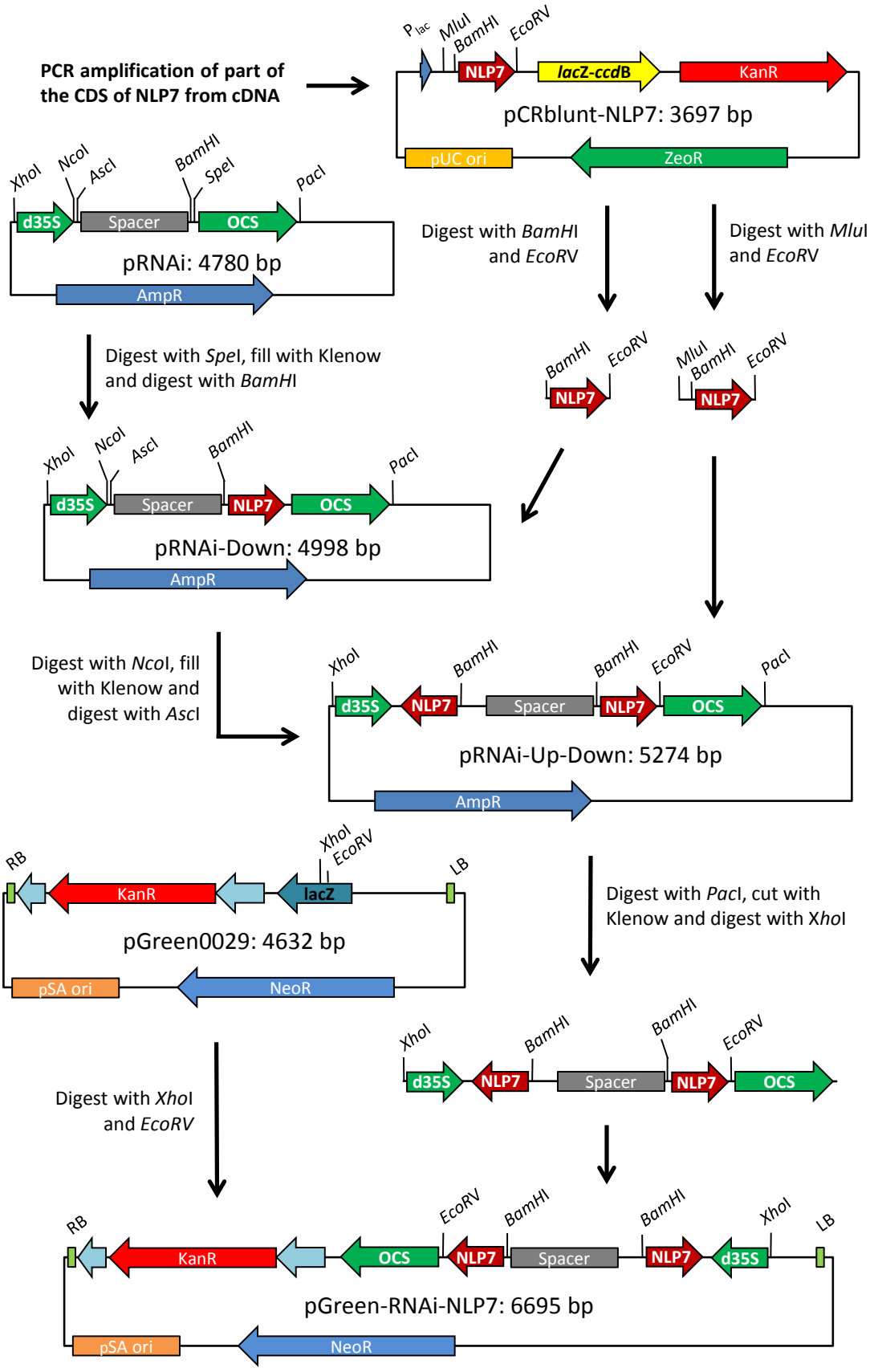

Figure 2.7.1. Cloning strategy for the construction of an RNA interference vector for *MtNLP7*.

First, a 185 bp sequence of the coding sequence of *MtNLP7* was amplified from the cDNA by PCR using the NLP7 primer pair (Table 2.2.1). The reaction was catalysed by the enzyme FideliTaq™ DNA Polymerase (usb®). The conditions of the PCR consisted in an initial denaturation (2 min at 94 ^{0}C), followed by 30 cycles of amplification (30 seconds at 94 ^{0}C; 30 seconds at 55 ^{0}C and 30 seconds at 68 ^{0}C) and a final extension of 5 min at 68 ^{0}C.

The PCR product was extracted from a 0.8% agarose gel, purified (Zymoclean™ Gel DNA Recovery Kit, Zymo Research Corp.) and ligated with 25 ng of linearized pCR®-Blunt using T4 DNA ligase (New England Biolabs® Inc., USA) with a 10:1 molar ratio over the vector. This vector aids the cloning process of blunt-end fragments given that the insertion site disrupts the expression of the *ccdB* gene, which encodes a potent gyrase inhibitor (Maki *et al.*, 1992) provoking cell death (Jaffe *et al.*, 1985). Thus, in ligated plasmids in the absence of insert, the expression of the CcdB protein leads to cell death, therefore establishing a selective pressure that favours blunt-end insertion. The ligated DNA was transformed into DH5α RbCl-competent cells and spread on an LB plate (5 g·L^{-1} yeast extract; 10 g·L^{-1} tryptone; 10 g·L^{-1} NaCl; 15 g·L^{-1} agar; pH 7.0) supplemented with kanamycin (50 µg·mL^{-1}).

Colony PCR was used to assay for positive recombinants. Random colonies were selected and dissolved in 100 µL of sterile H_2O and 8 µL were used as template in a 25 µL PCR reaction, catalysed by *Taq* DNA Polymerase (Sigma-Aldrich®) according to the instructions of the manufacturer. Two pairs of primers were used: the M13 primers, which yields a fragment of 424 bp in case of insertion of the *MtNLP7* fragment, and the NLP7 reverse and M13 reverse primers, which produce a 314 bp fragment only when in the insert is inserted in the sense orientation in respect to the vector. The conditions of the PCR were the following: initial denaturation (10 min at 94 ^{0}C), followed by 30 cycles of amplification (2 minutes at 94 ^{0}C; 30 seconds at 55 ^{0}C and 30 seconds at 72 ^{0}C) and a final extension of 5 minutes at 72 ^{0}C. At the end of the reaction, the PCR products were resolved in a 0.8% agarose gel and a positive clone was grown overnight in LB with kanamycin (50 µg·mL^{-1}). The pCRblunt-NLP7 plasmid was extracted using the ZR Plasmid Miniprep™-*Classic* (Zymo Research Corp.). This plasmid was digested in two parallel reactions to create a *BamH*I-NLP7-*EcoR*V and a *Mlu*I-NLP7-*EcoR*V fragments (New England Biolabs® Inc., USA). These bands were extracted from a 0.8% agarose gel and purified (Zymoclean™ Gel DNA Recovery Kit, Zymo Research Corp.).

In parallel, the pRNAi plasmid was obtained from an overnight culture (ZR Plasmid Miniprep™-*Classic*, Zymo Research Corp.) and digested overnight with *Spe*I (New England Biolabs® Inc., USA), treated with Klenow (Roche, Germany) to create a blunt end and digested with *BamH*I (New England Biolabs® Inc., USA). The result of this reaction was extracted from a 0.8% agarose gel and purified (Zymoclean™ Gel DNA Recovery Kit, Zymo Research Corp.). This

restricted vector was ligated overnight with the *BamH*I-NLP7-*EcoR*V fragment (T4 DNA ligase, New England Biolabs® Inc., USA), transformed into DH5α RbCl-competent cells and spread on an LA plate supplemented with ampicillin (100 μg·mL^{-1}). Positive clones were selected through colony PCR, as described above, using the NLP7 pair of primers. One clone was selected, grown overnight in LB with ampicillin (100 μg·mL^{-1}), to which followed the extraction of the pRNAi-Down plasmid (ZR Plasmid Miniprep™-*Classic*, Zymo Research Corp.). The insertion and orientation of the insert was further confirmed by restriction using the enzyme *Pst*I (New England Biolabs® Inc., USA).

The pRNAi-Down plasmid was then digested with *Nco*I (New England Biolabs® Inc., USA), treated with Klenow (Roche, Germany) to create a blunt end, extracted from a 0.8% agarose gel and purified (Zymoclean™ Gel DNA Recovery Kit, Zymo Research Corp.). The purified fragment was further digested overnight with *Asc*I (New England Biolabs® Inc., USA) and again extracted and purified from a 0.8% agarose gel. This restricted vector was ligated overnight with the *Mlu*I-NLP7-*EcoR*V fragment (T4 DNA ligase, New England Biolabs® Inc., USA), transformed into DH5α RbCl-competent cells and spread on an LA plate supplemented with ampicillin (100 μg·mL^{-1}). Twenty-four colonies were selected and overnight cultures were prepared. Plasmid DNA was extracted using the alkaline method and clones were screened by overnight digestion with *Kpn*I's isoschizomer *Acc*65I and *Sac*I (two independent restriction reactions; New England Biolabs® Inc., USA). Upon confirmation, the pRNAi-Up-Down plasmid was extracted from an overnight culture using the ZR Plasmid Miniprep™-*Classic* kit (Zymo Research Corp.) and the restriction pattern was again confirmed.

The pRNAi-Up-Down plasmid was then digested with *Pac*I (New England Biolabs® Inc., USA), treated with Klenow (Roche, Germany) to create a blunt end, extracted from a 0.8% agarose gel and purified (Zymoclean™ Gel DNA Recovery Kit, Zymo Research Corp.). The purified fragment was further digested overnight with *Xho*I (New England Biolabs® Inc., USA) and the band corresponding to a molecular weight of 2397 bp was again extracted and purified from a 0.8% agarose gel (Zymoclean™ Gel DNA Recovery Kit, Zymo Research Corp.).

In parallel, the pGreen0029 plasmid was obtained from an overnight culture (ZR Plasmid Miniprep™-*Classic*, Zymo Research Corp.) and digested overnight with *Xho*I and *EcoR*V (New England Biolabs® Inc., USA). The result of this reaction was extracted from a 0.8% agarose gel and purified (Zymoclean™ Gel DNA Recovery Kit, Zymo Research Corp.).

This restricted vector was ligated overnight with the *Xho*I-RNAi-NLP7 fragment (T4 DNA ligase, New England Biolabs® Inc., USA), transformed into DH5α RbCl-competent cells and spread on an LA plate supplemented with kanamycin (50 μg·mL^{-1}), IPTG (0.1 mM) and X-gal (40 μg·mL^{-1}), in order to allow screening of positive clones through α-complementation (white

colonies were selected). The final pGreen-RNAi-NLP7 plasmid was extracted (ZR Plasmid Miniprep™-*Classic*, Zymo Research Corp) and restricted in parallel with *Spe*I and *Hind*III (New England Biolabs® Inc., USA), to confirm the success of the cloning process.

2.8. *Agrobacterium rhizogenes*-mediated transformation

The pGreen-RNAi-NLP7 plasmid was transformed into *A. rhizogenes* competent cells as described in Chapter 2.10. A positive clone was selected and grown on TY solid medium (10 $g \cdot L^{-1}$ yeast extract; 16 $g \cdot L^{-1}$ tryptone; 5 $g \cdot L^{-1}$ NaCl; 15 $g \cdot L^{-1}$ agar; pH 7.0) at 28 ^{0}C.

After approximately 30 h germination, when seedlings had a radicle length of approximately 10 mm, the radicle was sectioned approximately 3 mm from the root tip with a sterile scalpel. Sectioned radicles were inoculated by coating the freshly cut surface with the *A. rhizogenes* grown on TY solid medium. The inoculated sectioned seedlings were placed on slanted agar (1.5%) containing a modified Fahraeus medium (0.9 mM $CaCl_2$, 0.5 mM $MgSO_4$, 0.7 mM KH_2PO_4, 0.8 mM Na_2HPO_4, 0.02 mM FeEDTA, 0.5 mM NH_4NO_3, supplemented with 0.1 $mg \cdot L^{-1}$ of $MnSO_4$, $CuSO_4$, $ZnCl_2$, H_3PO_4 and Na_2MoO_4) in square petri dishes. The petri dishes containing the inoculated seedlings were partially sealed (several incisions in the parafilm seal allowing gas exchange), placed vertically in a growth chamber for 12 days (16 h light (20 ^{0}C)/8 h dark (19 ^{0}C) cycles, with a light intensity of 200 µE per $s \cdot m^{-2}$) to optimize the transformation frequency. After twelve days, the temperature was increased to 25 ^{0}C and after 20 days they were grown aeroponically (section 2.1.1).

2.9. Preparation and transformation of RbCl competent DH5α cells

2.9.1. Preparation protocol

Competent cells were prepared following the RbCl protocol. 200 mL of YETM medium (5 $g \cdot L^{-1}$ yeast extract; 20 $g \cdot L^{-1}$ tryptone; 40 mM $MgSO_4 \cdot 7H_2O$; pH 7.5) were inoculated with 4 mL of an overnight culture prepared from a freshly streaked colony. Cultures were incubated at 37 ^{0}C with shaking and growth was monitored by measuring the optical density (590 nm) until an O. D. of 0.6. Cultures were chilled on ice for 10 to 15 minutes, centrifuged for 10 minutes (2000 rpm; 4 ^{0}C), gently resuspended in 10 mL of ice-cold TFB1 (30 mM KOAc; 100 mM RbCl; 10 mM $CaCl_2 \cdot 2H_2O$; 50 mM $MnCl_2 \cdot 4H_2O$; 15% glycerol; pH 5.8) and incubated on ice for 5 minutes.

Subsequently, the cells were centrifuged a second time under the previously mentioned conditions and resuspended in 2 mL of ice-cold TFB2 (10 mM MOPS; 10 mM RbCl; 75 mM $CaCl_2 \cdot 2H_2O$; 15% glycerol; pH 6.5). After a 15-minute incubation period on ice, cells were divided amongst several aliquots that were flash frozen in liquid nitrogen and stored at -80 ^{0}C. Competency efficiency was determined by transformation with 0.1 ng of pUC19 and counting the number of CFUs on a LB plate with 100 $\mu g \cdot mL^{-1}$ ampicillin after overnight incubation, which yielded 1.11 x 10^7 $CFUs \cdot \mu g^{-1}$ of DNA. Untransformed cells were also spread on LB plates supplemented with ampicillin (100 $\mu g \cdot mL^{-1}$) or kanamycin (50 $\mu g \cdot mL^{-1}$) and no colonies were observed after overnight incubation.

2.9.2. Transformation protocol

The amount of DNA to be transformed (10 to 100 ng) was added to 100 µL of RbCl competent cells, which had previously been thawed on ice. The mixture was initially incubated on ice for 20 to 30 minutes, heat-shocked for 90 seconds at 42 ^{0}C and subsequently incubated on ice for 2 minutes. 1 mL of LB medium was added and the culture was allowed to recover for 1 hour at 37 ^{0}C with gentle shaking, before being spread on a plate and selected with the appropriate antibiotic.

2.10. Preparation and transformation of *A. rhizogenes* competent cells

2.10.1. Preparation protocol

A. rhizogenes was grown overnight at 28 ^{0}C in TY medium. A 50 mL culture in TY was prepared using 2 mL of the overnight culture and incubated at 28 ^{0}C with shaking until an O. D. of 0.5-1.0. Cultures were chilled on ice for 10 to 15 minutes, centrifuged for 5 minutes (3000 g; 4 ^{0}C), gently resuspended in 1 mL of ice-cold 20 mM $CaCl_2$ and divided amongst several 100 µL aliquots that were flash frozen in liquid nitrogen and stored at -80 ^{0}C.

2.10.2. Transformation protocol

An aliquot of *A. rhizogenes* competent cells was thawed on ice and 1 µg of pGreen-RNAi-NLP7 and 1 µg of pSoup were added. The mixture was initially incubated on ice for 5 minutes, to which followed a 5-minute incubation in liquid nitrogen and a 5-minute incubation at 37^{0}C. Subsequently 1 mL of TY medium was added and the culture was allowed to recover

for 4 hours at 28 ^{0}C with gentle shaking, before being spread on a plate and selected with streptomycin (600 µg·mL^{-1}), kanamycin (50 µg·mL^{-1}) and tetracycline (10 µg·mL^{-1}).

2.11. Accession numbers and sequence analysis methodology

The complete coding sequences of *MtAMT3, MtNR3* and *MtNLP7* were obtained from GenBank (Benson *et al.*, 2012) following the accession numbers XM_003630338.1, XM_003601063 and XM_003592222.1, respectively. The number and relative position of introns/exons were determined through an alignment of the coding sequences and the genomic sequences of each gene, using the Serial Cloner software (Version 2.5, available online in: http://serialbasics.free.fr/Serial_Cloner.html). This software was also employed to perform *in silico* translation, while domain predictions were performed using the SMART (Simple Modular Architecture Research Tool) software (Version 7, accessible online in: http://smart.embl-heidelberg.de/) (Schultz *et al.*, 1998; Letunic *et al.*, 2012). The NetNES 1.1 Server (accessible online in: http://www.cbs.dtu.dk/services/NetNES/) was used to predict the presence of leucine-rich nuclear export signals (NES) (la Cour *et al.*, 2003).

Transmembrane regions of MtAMT3 were predicted by averaging the outputs of a number of hydrophobicity analysis programs, namely TOPPRED (von Heijne, 1992), HMMTOP (Tusnady and Simon, 1998; 2001) and TMHMM (Krogh *et al.*, 2001).

The multiple alignment of the amino acidic sequences of the members of the AMT family was performed using the ClustalW program (Larkin et al., 2007) and the sequences' accession numbers are indicated in Figure 3.2.3.

Chapter III

Results

3.1. Transcription profile of *MtAMT3*, *MtNLP7* and *MtNR3*

Data available in online databases regarding the expression profile of a multitude of transcripts under different conditions are undeniably helpful in the study of a particular gene, not only for it provides clues regarding gene function, but also because it aids in the experimental design. The *Medicago truncatula* Gene Expression Atlas (*Mt*GEA) is one of such tools, which organizes the expression data obtained from Affymetrix® GeneChip experiments made publicly-available (Benedito *et al.*, 2008; He *et al.*, 2009). In Figure 3.1.1, the transcription profile of *MtAMT3*, *MtNLP7* and *MtNR3* is represented.

As can be seen in the picture, the expression of *MtAMT3* is circumscribed to roots and nodules, responding to the auxin 1-naphthaleneacetic acid (NAA) in leaves, and appears not to be expressed in any other plant organ. In nodules, a 2-day treatment with NO_3^- reduces its level of expression to approximately 55% of that observed in mature nodules (14-days post infection (dpi) with rhizobium). In split roots the response to NO_3^- is similar, increasing from roots with sufficient NO_3^- to roots with limited and no NO_3^-. A similar pattern is observed when roots are treated with NH_4^+. In an experiment using split nodulated roots, in which one part of the roots were grown under limited N_2, and the other under normal N_2 atmosphere, the expression of *MtAMT3* is 2.5 times higher under limited N_2

Regarding the expression profile of *MtNR3*, the most striking characteristic is that this transcript appears to be nodule-specific, and its expression increases during nodule development achieving its maximal expression at 14-dpi. After 28 days, the expression of this transcript is completely abrogated. It too varies drastically in response to N status, as can be seen by the fact that a 2-day treatment with NO_3^- reduces its level of expression to approximately 30% of that observed in mature nodules (14-dpi). Similarly to *MtAMT3*, in

nodulated split roots grown in a limited N_2 atmosphere, the expression of *MtNR3* is 1.7 times higher than control.

When it comes to *MtNLP7*, and unlike the above mentioned genes, its expression is more global, as it is detected in all plant organs represented, except pods, having its maximum expression in leaves. In nodules, its expression decreases as the nodule matures, from 4-dpi to 10-dpi, 14-dpi and 28-dpi. In this same organ, and unlike the two previously mentioned genes, the expression of *MtNLP7* increases 60% after treatment with NO_3^-. Interestingly, in split roots, the response to treatment with NO_3^- appears to be the opposite to that observed in nodules, for its expression diminishes with increasing quantities of NO_3^-. The expression of this transcript did not vary in nodulated split roots grown in a limited N_2 atmosphere, when compared to normal conditions. Finally, its expression increases 25% when the plant is grown in symbiosis with arbuscular mycorrhizal fungi, which provides inorganic phosphorous and nitrogen to the plant in exchange for carbon (Gomez *et al.*, 2009).

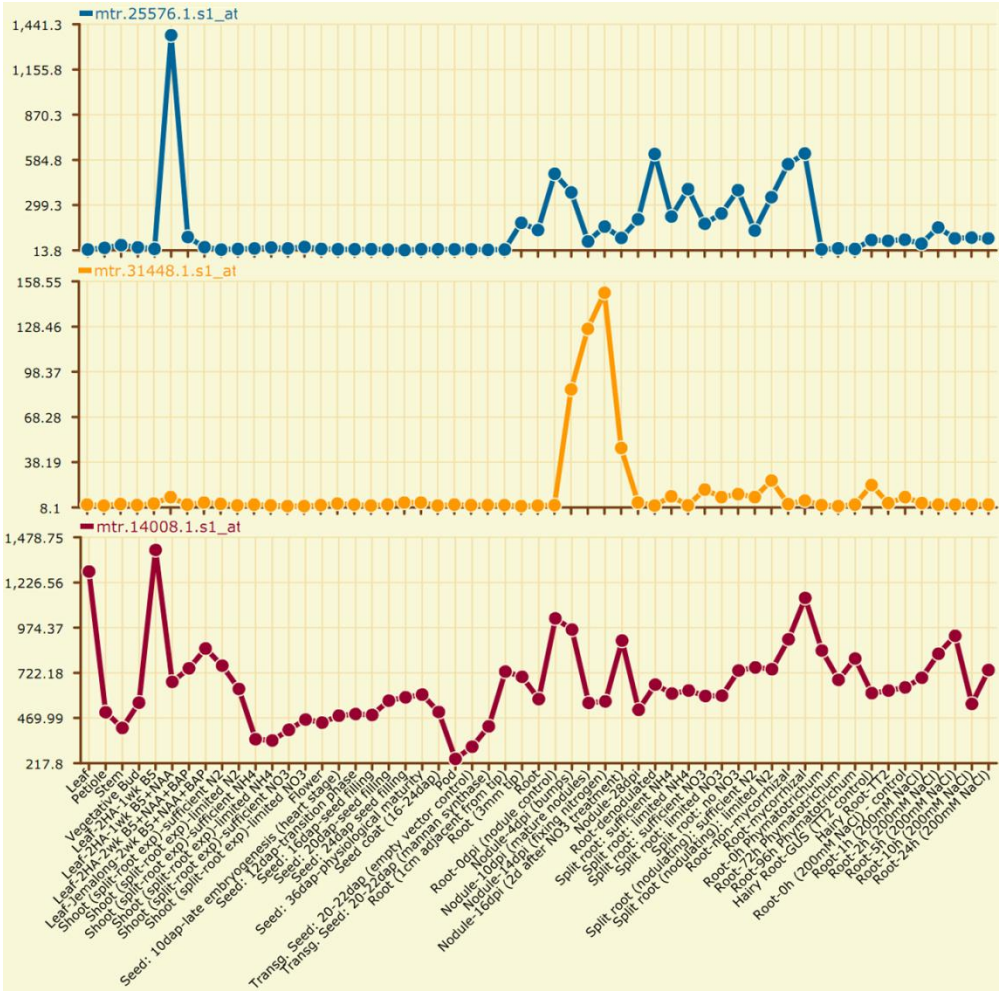

Figure 3.1.1. Expression profile of the *MtAMT3* (top), *MtNR3* (centre) and *MtNLP7* (bottom) transcripts as given by *Mt*GEA. Probe IDs are, respectivelly, mtr.25576.1.s1_at, mtr.31448.1.s1_at and mtr.14008.1.s1_at.

3.2. Characteristics of the *MtAMT3*, *MtNLP7* and *MtNR3* sequences

3.2.1. *MtAMT3*, *MtNR3* and *MtNLP7* gene structure

In order to characterize the genes under study, the genomic sequence and the predicted coding sequence were aligned so that the number and relative position of the exons in these genes could be determined. The results are summarized in Figure 3.2.1.

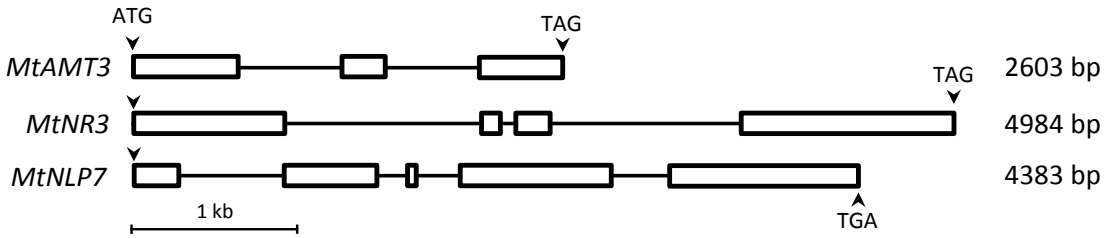

Figure 3.2.1. *MtAMT3*, *MtNR3* and *MtNLP7* gene structures. Arrowheads show initiation (ATG) and termination codons. Boxes depict the exon regions.

MtAMT3 has a simple structure composed of three exons and two introns, whilst *MtNR3* has four predicted exons and three introns and *MtNLP7* is composed of five exons and four introns.

3.2.2. Sequence analysis, topology prediction and classification of *MtAMT3*

The protein encoded by *MtAMT3* is predicted to have 485 amino acids and a molecular weight of 52.2 kDa. The amino acidic sequence was analysed using topology prediction programs that make assignments based on a combination of hydrophobicity and topogenic signals located within the primary amino acid sequence, namely TOPPRED (von Heijne, 1992), HMMTOP (Tusnady and Simon, 1998; 2001) and TMHMM (Krogh *et al.*, 2001). The first of these programs is based solely in the hydrophobicity of the residues and in the observation that positively-charged amino acids are more abundant in cytoplasmic regions ("positive-inside" rule) (von Heijne, 1992). The remaining two programs use hidden Markov models to predict membrane topology, which can incorporate hydrophobicity, charge bias, helix length and grammatical constraints into one model (grammatical constraints refer to the fact that cytoplasmic and non-cytoplasmic loops have to alternate) (Krogh *et al.*, 2001).

The outputs of these programs were concordant and offered a high degree of certainty, as all predicted eleven transmembrane helices, interspersed with cytoplasmic and non-cytoplasmic domains, placing the N-terminus in the extracellular side of the membrane and C-terminus in the cytoplasm ($N_{OUT}C_{IN}$), as depicted in Figure 3.2.2. Besides the topology

just described, TOPPRED offered yet a second possibility, where an extra helix is present in the N-terminus. However, the probability for that particular helix was low and the first model was favoured and this is why in Figure 3.2.2 B helices are numbered from 2 to 12 (the low-probability helix 1 is not shown). These results are in agreement to the topology that has been proposed to characterize the AMT family of ammonium transporters (Thomas *et al.*, 2000).

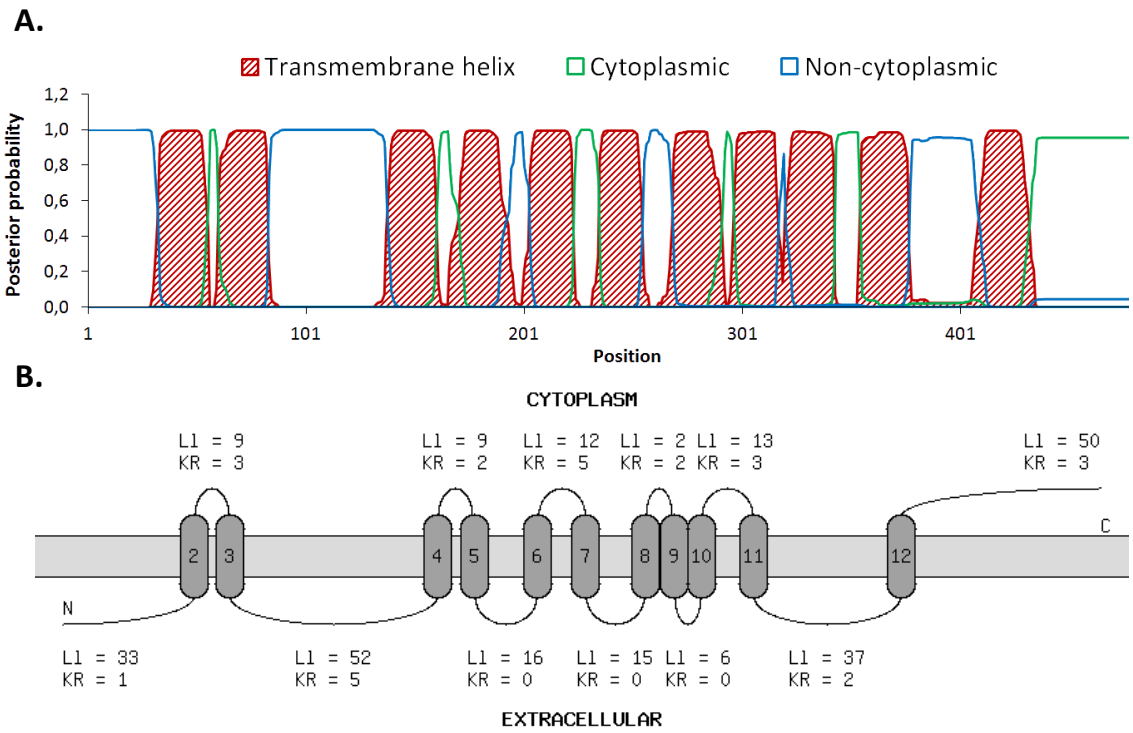

Figure 3.2.2. Membrane topology prediction of MtAMT3. **A.** Posterior probabilities for transmembrane, cytoplasmic or non-cytoplasmic amino acids calculated by the TMHMM algorithm. Eleven transmembrane helixes, six cytoplasmic and six non-cytoplasmic regions are predicted for this protein with a good degree of certainty (very high values for posterior probability). **B.** Membrane topology of MtAMT3 as predicted by the TOPPRED algorithm (Ll: loop length; KR: number of Lysine and Arginine residues (positively charged)).

As previously described, in plants ammonium transporters tend to be divided in two different families, according to their amino acid sequence. In order to characterize the ammonium transporter under study in this work, its sequence was aligned with that of several other ammonium transporters from *A. thaliana*, *L. japonicus*, *E. coli* and *S. cerevisiae*. Amino acid sequence comparison showed that MtAMT3 belongs to the family of the AMT2 proteins, which is distinct from the AMT1 transporters (Figure 3.2.3). The divergence of the two groups appears to be older than the emergence of eukaryotes, given that members of the AMT2 family are more similar to their prokaryotic homologues than they are to the AMT1 proteins of

the same species. MtAMT3 shares only 20% sequence identity with MtAMT1;1 (and between 19% and 21% with the *A. thaliana* and *L. japonicus* orthologues of the AMT1 family), yet shares 31% sequence identity with AmtB of *E. coli*, 70% with LjAMT2;1 and 65% with AtAMT2;1. For this reason, we propose *MtAMT3* to be classified as a member of the AMT2 family, and thus that its annotation should be corrected in the public databases.

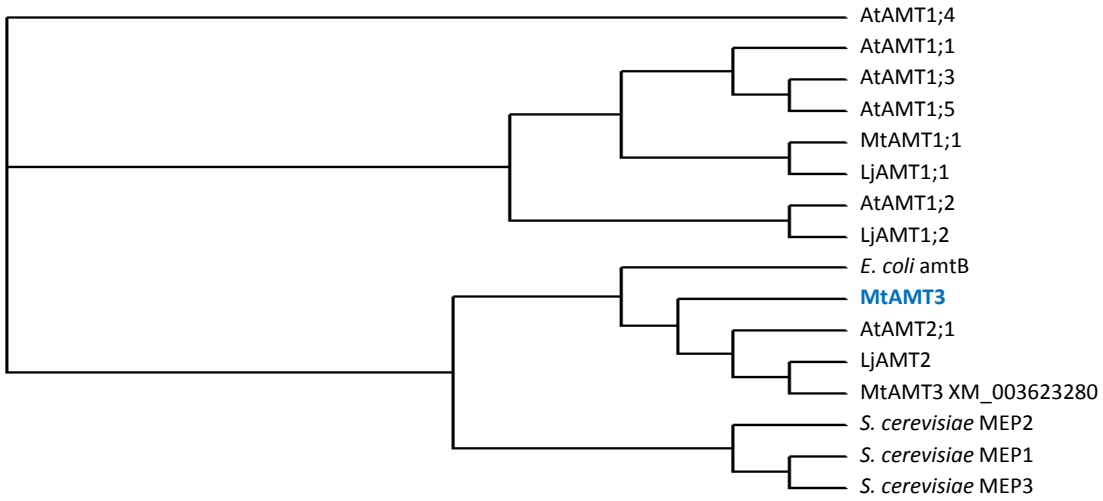

Figure 3.2.3. Distance tree of selected AMT proteins based on a ClustalW multiple alignment of amino acidic sequences (Neighbour joining method) (Larkin et al., 2007). Selected proteins include the prokaryotic AmtB of *E. coli* (AAD14837); the MEP proteins of *S. cerevisiae* (P40260, P41948 and P53390, for MEP1, MEP2 and MEP3, respectively); the members of the AMT1 (AEE83287, AEE34288, AEE76886, AEE85527 and AEE76885) and AMT2 (AEC09519) families of *A. thaliana* and the AMT1;1 (AF182188), AMT1;2 (AY135020) and AMT2;1 (AF187962.1) of *L. japonicus*. This tree includes also, from *M. truncatula*, the sequence of the AMT1;1 protein and the two sequences annotated in GenBank as AMT3, that is, the sequence under current study (highlighted in blue) and a second sequence with the accession number (XM_003623280).

Through a BLAST search in the GenBank database, a second and distinct sequence annotated as *MtAMT3* was found. The protein encoded by this second sequence shares 70% amino acid identity with the MtAMT3 protein under current study, which is less than what it shares with AtAMT2;1 (77%) and LjAMT2;1 (88%). Therefore, it is reasonable to propose that both proteins belong to the AMT2 family, which means that in *M. truncatula* this is a multigene family, fact that has not yet been observed in *A. thaliana* or in *L. japonicus*. These proteins have nevertheless distinct expression patterns, as can be seen in Figure 3.2.4, where data retrieved from *Mt*GEA are presented. While the expression of *MtAMT3* is circumscribed to

roots and nodules and responds to NAA in leaves, as previously described, the expression of the second transcript is global, being found in leaves, petioles, stems, shoots, flowers, seeds, roots and nodules. Additionally, the expression of this transcript did not vary with treatment with PPT (Seabra, A., personal communication), unlike the *MtAMT3* transcript under study. One can hypothesize that the root/nodule-specific *MtAMT3* exerts a distinct physiological role specific to this particular and specialized organ.

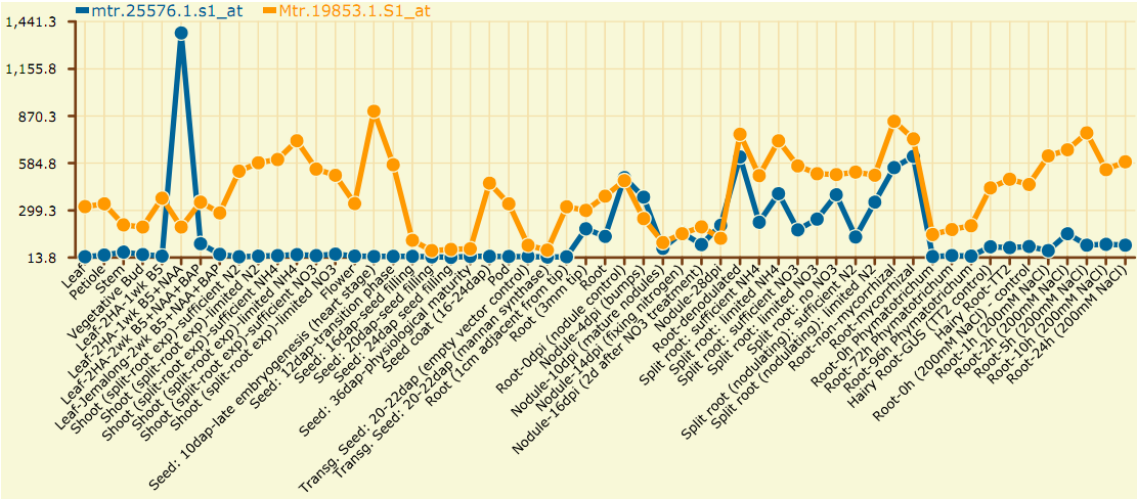

Figure 3.2.4. Expression profile of the *MtAMT3* transcripts as given by MtGEA. The gene under study in this work is depicted in **blue** (probe ID: mtr.25576.1.s1_at), while the second transcript is represented in **yellow** (mtr.19853.1.s1_at).

3.2.3. NR3 amino acid sequence is typical of a nitrate reductase

Nitrate reductases in higher plants are NADH-specific forms (EC 1.6.6.1) that act has homodimers composed of two monomers of ~100 kDa. *MtNR3* encodes a protein of 876 amino acids with an expected molecular weight of 99.1 kDa, which is predicted to contain several different functional domains typically found in NADH-specific nitrate reductases, as shown schematically in Figure 3.2.5.

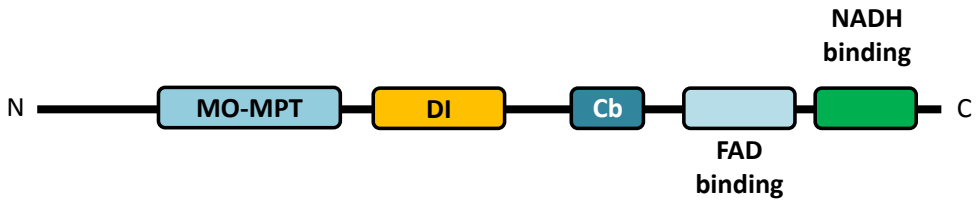

Figure 3.2.5. Schematic representation of the amino acid sequence of MtNR3. MO-MPT domain, residues 116-299. Dimer interface (DI) domain, residues 324-457. Cytochrome b (Cb) domain,

residues 518-591. FAD binding domain, residues 625-732 and NADH binding domain, residues 752-859. Domain predictions were made using the SMART (Simple Modular Architecture Research Tool) software.

It can be seen that the MtNR3 has the typical structure of a plant nitrate reductase, which has been described and reviewed elsewhere (Campbell, 1999). In particular, this enzyme possesses a Mo-molybdopterin (Mo-MPT) binding domain, which binds this cofactor and is the active site for nitrate reduction; a dimer interface (DI) domain, which allows the formation of stable dimers; a cytochrome b (Cb) domain, which binds the prosthetic group hæm; and finally binding domains for flavin adenine dinucleotide (FAD) and nicotinamide adenine dinucleotide (NADH).

3.2.4. NIN-like protein 7 contains domains typical of transcription factors

The deduced NLP7 protein of 979 amino acids with an expected molecular weight of 108.6 kDa is predicted to contain several different functional domains, as shown schematically in Figure 3.2.6.

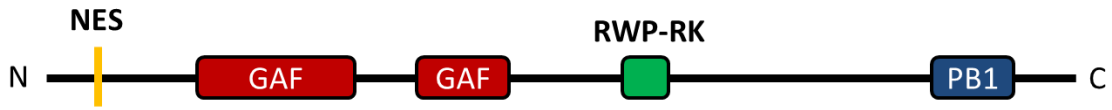

Figure 3.2.6. Schematic representation of the amino acid sequence of MtNLP7. Yellow bar, Leucine-rich NES, residues 28-32. GAF domains, residues 124-285 and 365-447. RWP-RK domain, residues 570-621 and PB1 domain, residues 883-966. Domain predictions were made using the SMART (Simple Modular Architecture Research Tool) software.

In the N terminus half of the protein, MtNLP7 contains two GAF domains such as those found in phytochromes (Aravind and Ponting, 1997) and cGMP-specific phosphodiesterases (Rybalkin *et al.*, 2003). In fact, the acronym stems from the fact that this domain was initially found in cGMP-specific phosphodiesterases, adenylate cyclases and the *E. coli* FhlA protein. This motif was found to bind cGMP and cAMP (Ho *et al.*, 2000; Kanacher *et al.*, 2002), and, interestingly, nitric oxide (NO) (D'Autreaux *et al.*, 2005). It was shown that the GAF domain in the transcription factor NorR binds NO and that this molecule does not activate transcription of genes involved in NO detoxification processes in the absence of this domain, which suggests that the GAF domain plays a role as a NO sensor in this system (D'Autreaux *et al.*, 2005). In

MtNLP7, the first GAF domain is divided between exons 2 and 3, while the second GAF domain in entirely encoded by exon 4.

Additional motifs in the protein sequence include a nuclear export signal (NES) upstream the first GAF domain and a PB1 (Phox and Bem1) domain, in the C terminus. The PB1 domain mediates the formation of complexes with other proteins containing PB1 domains, thus forming homo- or heterodimers (Noda *et al.*, 2003; Moscat *et al.*, 2006).

Finally, MtNLP7 contains also a RWP-RK domain, which is highly conserved across a variety of plant proteins and whose name stems from the presence of invariant amino acids in the consensus sequence. Its secondary structure was predicted to be an α-helical basic region followed by a helix–turn–helix and a helical leucine zipper, spaced by loops, which is similar to the ubiquitous basic leucine-zipper and helix–turn–helix classes of DNA-binding domains. For this reason, this domain was predicted to be involved in DNA binding (Schauser *et al.*, 1999; Schauser *et al.*, 2005), which has indeed been shown in the Nit2 protein from *C. reinhardtii*, an orthologous sequence to MtNLP7 (Camargo *et al.*, 2007). Interestingly, transcription factors with helix–turn–helix and helical leucine zippers tend to act as dimers, and thus the presence of the PB1 domain is not surprising. It is also entertaining to notice that this domain is divided between exons 4 and 5, thus one can reasonably hypothesise that alternative splicing can be used to control the activity of this protein, given that if either exon is not present, MtNLP7 will not have a functional DNA binding domain.

When compared to its orthologues, the RWP-RK domain found in *MtNLP7* is highly conserved (Figure 3.2.7). It shares 90% of amino acidic sequence identity with *AtNLP7*, a known transcription factor (Castaings *et al.*, 2009), fact that accentuates its likelihood to act as a transcription factor governing N sensing in *M. truncatula*.

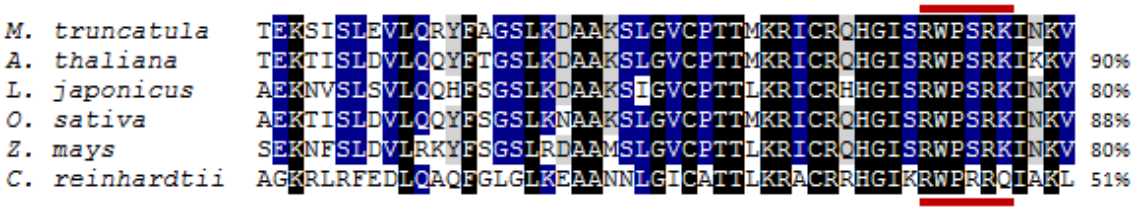

Figure 3.2.7. Alignment of the RWP-RK domain from NLP7 of *M. truncatula*, the Nit2 protein of *C. reinhardtii* (DQ311647) and several NIN-like plant proteins: NLP7 of *A. thaliana* (NM_118534.5), NLP2 of *Lotus japonicus* (CAE30325), *Oryza sativa* (BAD81274) and *Zea mays* (AAV64196). The RWP-RK sequence is underlined.

Finally and when analysed as a whole, the MtNLP7 amino acid sequence shows a DNA binding domain, an oligomerization domain and a possible signal-sensing region, a combination that is typical of transcription factors.

3.3. Fix^-, NO_3^--treated and *S. medicae*-inoculated nodules show differential expression of *MtAMT3*, *MtNR3* and *MtNLP7*

With the purpose of evaluating whether specific transcriptional variations occur in target genes in ineffective Fix^- nodules or in response to treatment with nitrate, as well as between *S. meliloti*- and *S. medicae*-mediated symbiosis, the expression profile of *MtAMT3*, *MtNR3* and *MtNLP7* was assayed by RT-qPCR under these different conditions. The specificity of the primers used and overall quality of the RT-qPCR results were assayed through analysis of the melting curves and gel electrophoresis (Figure 3.3.1). The integrity of the extracted RNA was assayed prior to its conversion to cDNA (Figure 3.3.1 A) and the stability of the reference gene was evaluated and shown to be steady across the conditions tested (Figure 3.3.1 B). The reference gene used was *elf1α*, for it has been shown that its expression is stable under different biological and physiological conditions in different species and it is routinely used as a reference gene in *M. truncatula* (Czechowski *et al.*, 2005; Nicot *et al.*, 2005; Jain *et al.*, 2006).

For each primer set, each reaction shows a sharp peak at the same melting temperature, which is indicative of single-product amplification (Figure 3.3.1 C1-C4). This observation was confirmed by gel electrophoresis (Figure 3.3.1 D1-D2), as for in each reaction only one band is seen and its size corresponds to the size of the expected amplified product (given in Table 2.2.1). Overall, this means that the primers used are specific for each respective gene and thus amplification of off-target sequences does not occur, assuring that differences in C_q values are indeed due to differences in the initial amounts of transcript in the sample and not to nonspecific amplification of other molecules.

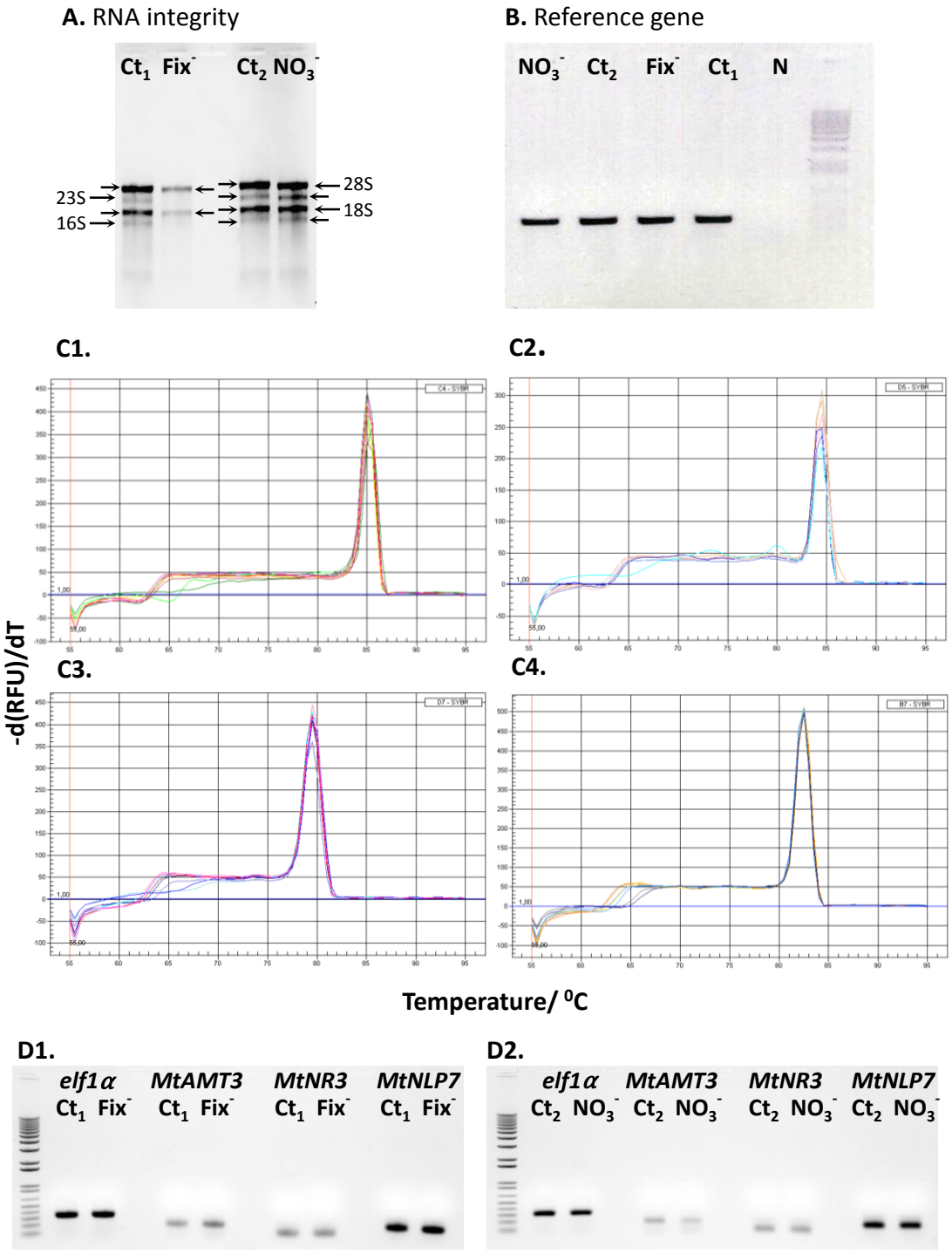

Figure 3.3.1. Analysis of the quality of the RT-qPCR results. **A.** Ethidium bromide stained 1% agarose gel of RNA samples extracted from control (Ct_1) and Fix^- root nodules and control (Ct_2) and NO_3^--treated root nodules. 28S and 18S bands correspond to the ribosomal RNA of the plant and 23S and 16S bands to the ribosomal RNA of the *Rhizobium*. **B.** Ethidium-bromide stained 0.8% agarose gel of PCR products of *elf1α* transcripts extracted from control (Ct_1) and Fix^- root nodules and control (Ct_2) and NO_3^--treated root nodules using equal amounts of cDNA (25 ng). N

– Negative control/absence of DNA template. **C1-C4** correspond to the melting curves of each group of samples per primer set (1 – *elf1α*; 2 – *MtAMT3*; 3 – *MtNR3*; 4 – *MtNLP7*). **D1-D2.** Ethidium bromide stained 0.8% agarose gel of the end-products of one of each duplicate of the RT-qPCR reactions. **D1** shows control and Fix^- samples and **D2** control and nitrate-treated samples.

The C_q values obtained allowed the calculation of the relative expression ratio of each gene under study between control and test samples, normalized according to the expression of the reference gene *elf1α*, following the model described by Pfaffl (2001). Results are shown in Figure 3.3.2.

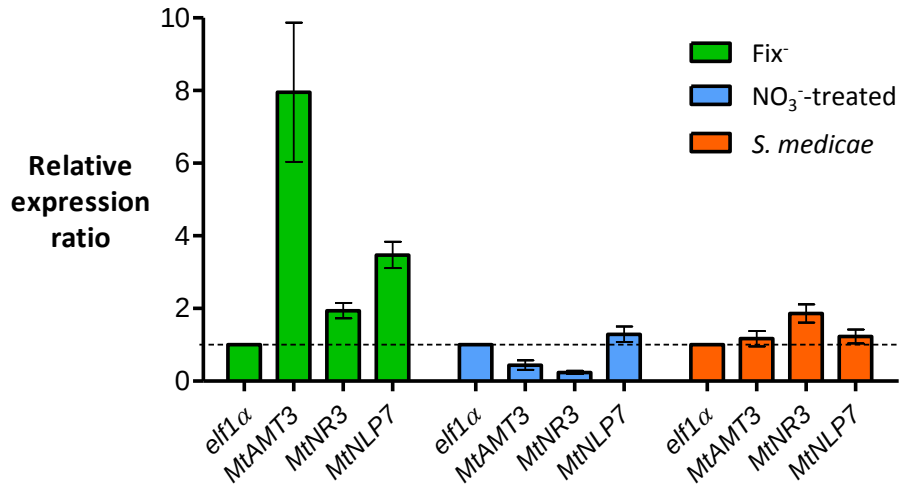

Figure 3.3.2. Quantification of *MtAMT3*, *MtNR3* and *MtNLP7* transcripts extracted from root nodules subjected to different N conditions by qPCR using equal amounts of cDNA (50 ng). The amount of transcript was normalized to that found in each control and using *elf1α* as a reference gene. Results are given as the relative expression ratio calculated from the mean of the C_q values of duplicate reactions with standard deviation, calculated from the standard deviation of the C_q values in accordance to the rules of error propagation.

It can be seen that all three target genes are overexpressed in Fix^- nodules in comparison to the control. *MtAMT3* shows the greatest increase in the expression level (approximately 8-fold), followed by *MtNLP7* (3.5-fold increase) and *MtNR3* (approximately 2-fold). This contrasts with the variations observed in NO_3^--treated nodules, as in this case the expression of *MtAMT3* and *MtNR3* are quantified as 0.44 and 0.24 in relation to control nodules, respectively, which corresponds to a downregulation of two-fold and four-fold. The expression of *MtNLP7*, conversely, is increased by 1.3-fold in NO_3^--treated nodules. Finally,

juxtaposing both controls allows the comparison between the symbioses established with either *S. meliloti* or *S. medicae*, which is a better N fixer, in terms of expression of the target genes. *MtAMT3* and *MtNLP7* do not vary greatly, but a 1.9-fold increase is observed in the expression of *MtNR3*.

Although this represents a single independent experiment, where pools of different individuals were used, these preliminary results were further confirmed by standard PCR, as shown in Figure 3.3.3. Qualitative differences can be detected in the intensity of the amplified bands, which support the results presented above, namely overexpression of *MtAMT3*, *MtNR3* and *MtNLP7* in Fix^- nodules, decreased expression of *MtAMT3* and *MtNR3* in NO_3^--treated nodules and overexpression of *MtNR3* in nodules formed by *S. medicae*. The formation of a secondary band when using specific primers for *MtNLP7*, which is smaller than 100 bp, corresponds to primer-dimer formation.

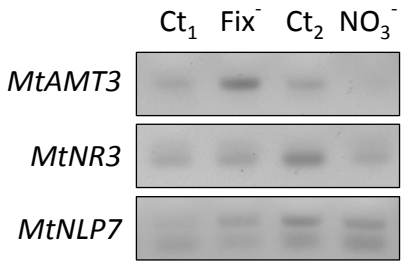

Figure 3.3.3. Ethidium-bromide stained 0.8% agarose gel of PCR amplification products of *MtAMT3*, *MtNR3* and *MtNLP7* transcripts extracted from control (Ct_1) and Fix^- root nodules and control (Ct_2) and NO_3^--treated root nodules using equal amounts of cDNA (30 ng).

3.4. *MtAMT3* and *MtNLP7* respond to variations of the N status in seedlings

In order to verify whether there are specific responses of *MtAMT3* and *MtNLP7* to different nitrogen sources, seedlings grown for three weeks solely on agar (and thus in nitrogen deficiency) were treated with KNO_3 and $NH_4H_2PO_4$, to assay, respectively, the effects of nitrate and ammonium. Seedlings were harvested both 3 and 24 hours after the start of treatment in order to detect both immediate and delayed responses. The root and aerial organs of the seedlings were analysed separately. RNA was extracted from pools of nine independent individuals for each of the conditions tested, converted to cDNA and the

expression of *MtAMT3* and *MtNLP7* was analysed through semi-quantitative PCR (Figure 3.4.1). The expression of *MtNR3* was not assayed given that this transcript is predicted to be nodule-specific, as described in Chapter 3.1.

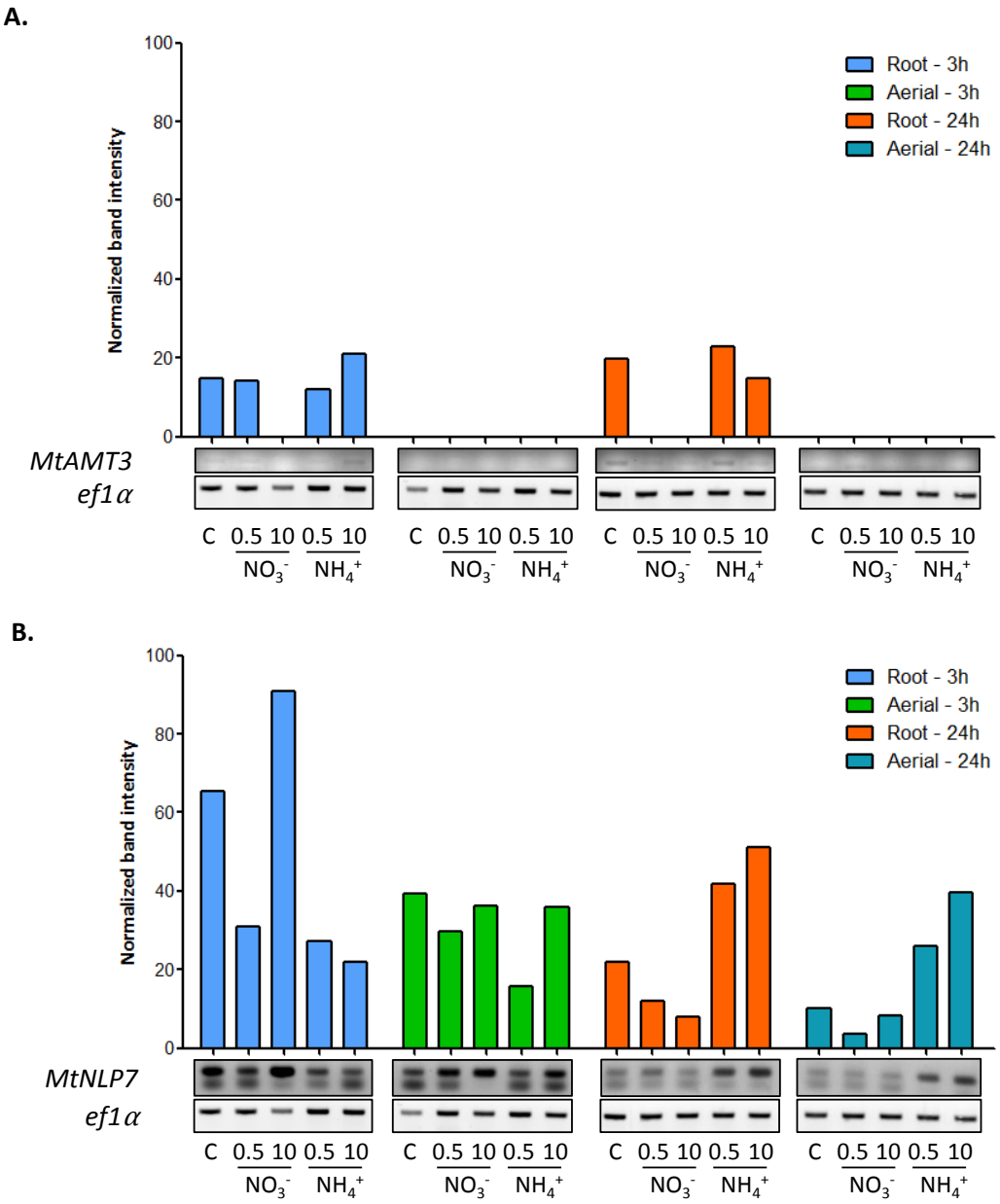

Figure 3.4.1. Evaluation of the expression of *MtAMT3* (**A**) and *MtNLP7* (**B**) in three-week old seedlings of *M. truncatula* grown under different N nutrition conditions by semi-quantitative PCR using 30 ng of template cDNA. Treatments were: phosphate buffer (C, control), 0.5 or 10 mM KNO_3, or 0.5 or 10 mM $NH_4H_2PO_4$, in phosphate buffer. Total RNA was extracted from pools of 9-10 individuals, separating roots and the aerial parts, 3 or 24 hours after the start of the treatment (arbitrary units).

The expression of *MtAMT3* was not detectable in the aerial organs of the seedlings, at any given time point, as expected. In roots, it was upregulated in response to 10 mM ammonium at 3h and 0.5 mM ammonium at 24h. Nitrate treatment seems to abrogate the expression of *MtAMT3* at 3h (10 mM) and 24h (both 0.5 mM and 10 mM). Nevertheless, these results need to be interpreted with caution, since band intensities are fairly low and this method is not the ideal to quantify gene expression. For this reason, the variations described should be confirmed by RT-qPCR.

MtNLP7 is upregulated in roots in response to 10 mM nitrate after 3h, yet downregulated in response to a lower nitrate concentration, as well as to ammonium treatment. In the aerial organs, no significant differences are seen between treatments and control, except a decrease in response to 0.5 mM ammonium. After 24h, the induction appears to occur in response to ammonium and not to nitrate, in both organs.

Overall, these results suggest that both genes respond to variations in the N nutrition and can thus be seen either as sensors of N status or as coordinators of the plant's response to environmental N cues.

3.5. Variation of GS expression, protein content and activity in response to the N status in seedlings

To investigate whether GS enzymes are regulated by nitrate or ammonium, the expression of *MtGS1a*, *MtGS1b* and *MtGS2a* was assayed by semi-quantitative PCR in seedlings grown different N sources, as described above. This analysis was further deepened by examining variations occurring at the protein level, namely by quantifying total GS activity in crude protein extracts and protein content by western blotting against polyclonal GS antibodies.

Figure 3.5.1 shows the variation in expression of the three main GS genes of *M. truncatula* (the expression of *MtGS2b* was not analysed, given that it is seed-specific). Band intensities were measured, normalized against that of the reference gene in the same condition (*elf1α*) and used to calculate the relative expression ratio, by dividing the value of test samples by the value of the respective control. These values are presented in Table 3.5.1.

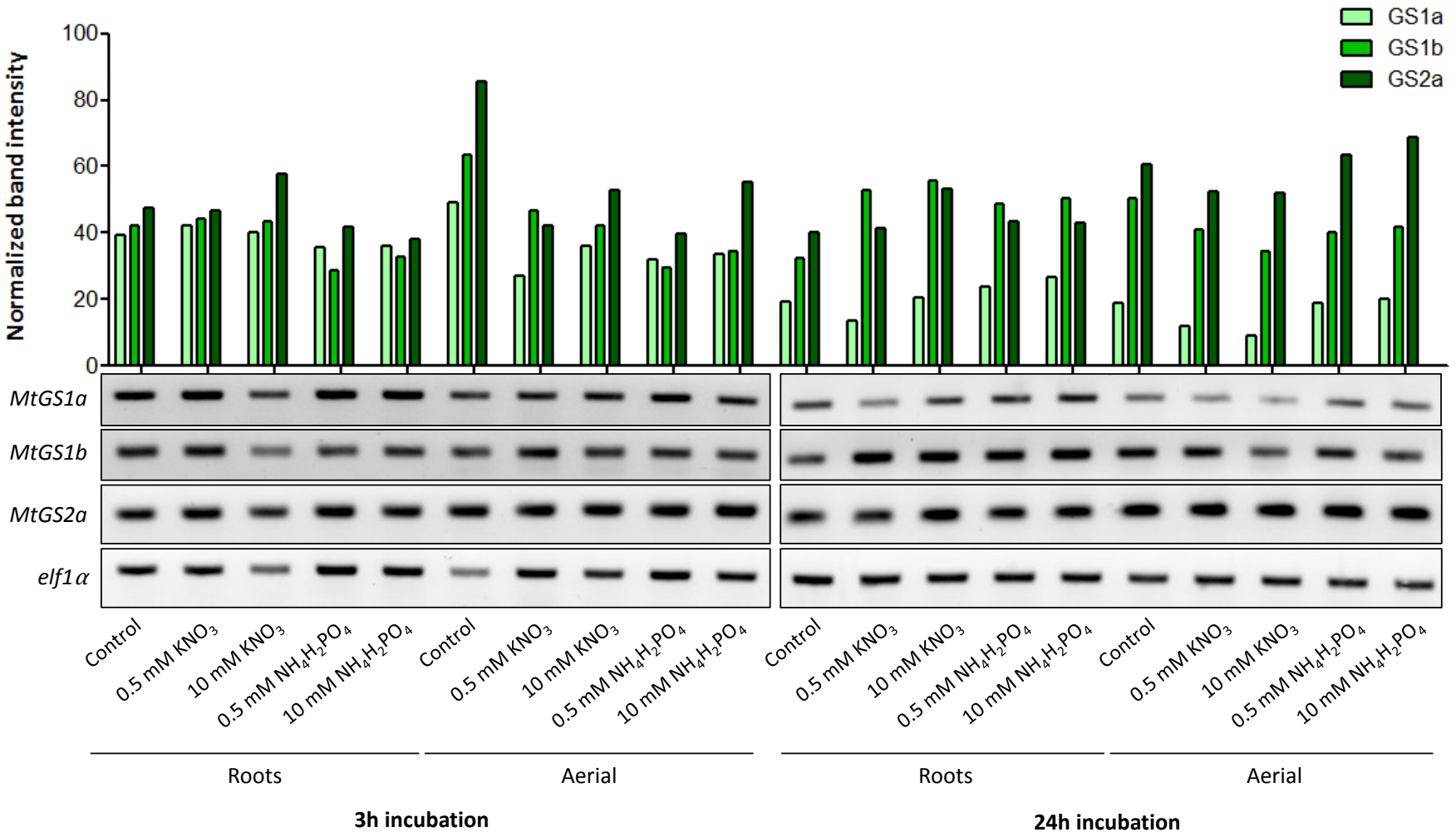

Figure 3.5.1. Evaluation of *MtGS1a*, *MtGS1b* and *MTGS2a* expression in three-week old seedlings of *M. truncatula* under different N nutrition conditions by semi-quantitative PCR using 30 ng of template cDNA (arbitrary units). Treatment varied from phosphate buffer (control), 0.5 or 10 mM KNO_3 or 0.5 and 10 mM $NH_4H_2PO_4$, in phosphate buffer. Total RNA was extracted from pools of 9-10 individuals, separating roots and the aerial parts, 3 or 24 hours after the start of the treatment.

Table 3.5.1. Relative expression ratio of *MtGS1a*, *MtGS1b* and *MtGS2a* in roots and aerial organs of three-week old seedlings after 3h and 24h of treatment with 0.5 or 10 mM KNO_3 or 0.5 and 10 mM $NH_4H_2PO_4$ in phosphate buffer, normalized according to the control condition (treatment with phosphate buffer)

Treatment		Time and organ											
		3 hours						24 hours					
		Roots			Aerial			Roots			Aerial		
KNO_3	0.5 mM	1,07	1,05	0,99	0,55	0,74	0,49	0,69	1,62	1,03	0,63	0,81	0,86
	10 mM	1,02	1,02	1,21	0,74	0,67	0,62	1,07	1,71	1,33	0,49	0,69	0,86
$NH_4H_2PO_4$	0.5 mM	0,91	0,68	0,88	0,65	0,47	0,47	1,22	1,50	1,08	1,00	0,80	1,05
	10 mM	0,91	0,77	0,81	0,69	0,55	0,65	1,37	1,55	1,07	1,06	0,83	1,13
		GS1a	GS1b	GS2a	GS1a	GS1b	GS2a	GS1a	GS1b	GS2a	GS1a	GS1b	GS2a

Clear tendencies in GS expression in response to the different nitrogen sources were not seen. In roots and after 3 hours of treatment, the expression of *MtGS1a* does not seem to vary significantly, while *MtGS1b* and *MtGS2a* seem to be slightly downregulated in response to both 0.5 and 10 mM NH_4^+. The expression of *MtGS2a* is induced in response to 10 mM KNO_3, but not to 0.5 mM KNO_3. In the aerial part of the plant, however, the higher expression of all genes in the control sample, as opposed to the nitrogen treatments, was noteworthy, suggesting an apparent inhibition of all GS genes in the photosynthetic tissues in response both to NO_3^- and NH_4^+.

After 24 hours of N treatment, in roots, there appears to be an overall induction of *MtGS1b* and a small induction of *MtGS1a* in response to 10 mM NH_4^+. The expression of *MtGS2a*, on the other hand, does not vary greatly, except in response to 10 mM NO_3^-. In the photosynthetic organs, the only distinguishable variation occurs in the expression of *MtGS1a*, which is downregulated in response to 10 mM NO_3^-.

Overall, the expression of the GS genes does not seem to be significantly affected by the N-source, since only slight variations were observed between each set of conditions. However, when analysing the GS activity and GS polypeptide content, significant variations were found, especially at 3 hours of treatment. Figure 3.5.2 A shows a representative western blot of total soluble proteins extracted from the roots and aerial parts of control and treated seedlings after 3 and 24 hours. The most striking variations are seen after 3 hours. In roots there seems to be a higher amount of GS, most prominently GS2, in seedlings treated with 10 mM NO_3^- and 10 mM NH_4^+, with a stronger induction in the latter. Interestingly, when the same substrates are provided at submillimolar concentrations, the levels of GS are reduced when compared to the control. In the photosynthetic tissues, the pattern is very similar. This

pattern was also observed in roots, but not in the aerial organs, in terms of GS activity (Figure 3.5.2 B). In fact, in aerial organs, higher concentrations of NO_3^- and NH_4^+ led to a small decrease in activity of GS. These data point to a differential and opposite response of GS in function of the concentration of the provided N substrate. Moreover, the differences observed between protein quantity and GS activity suggest the effect of a posttranslational modification.

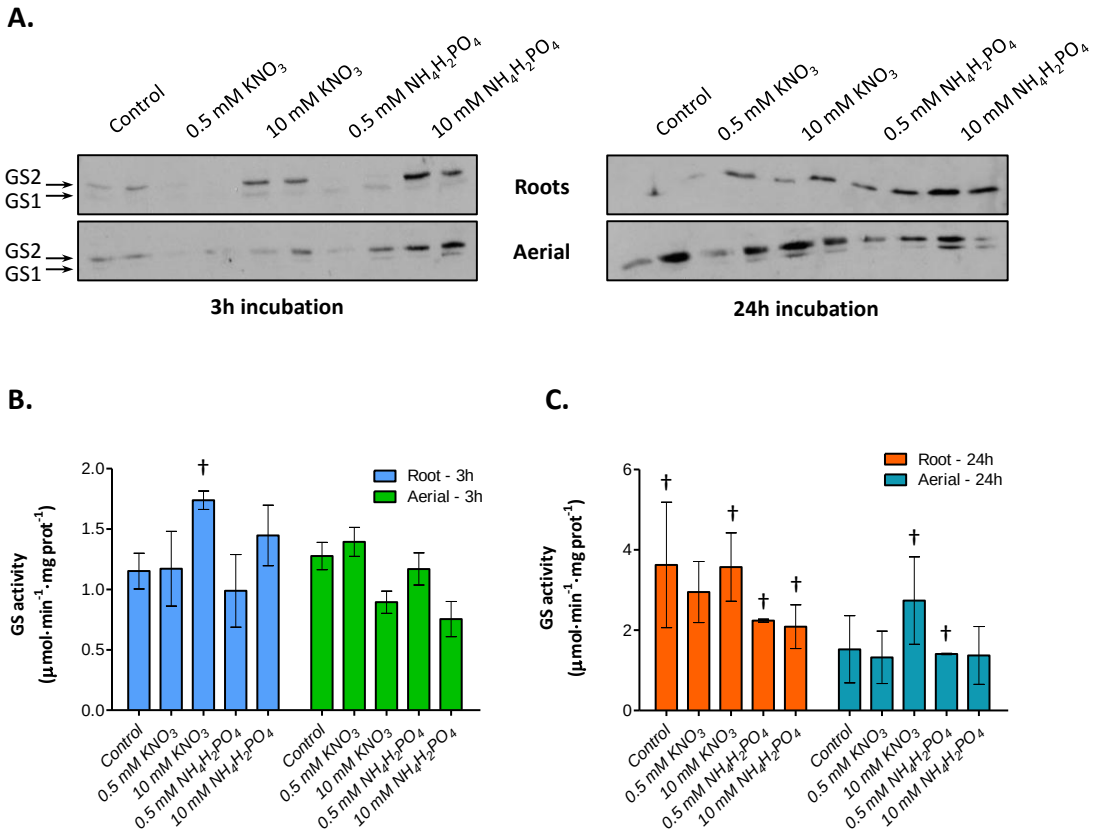

Figure 3.5.2. Evaluation of GS protein content and activity in three-week old seedlings of *M. truncatula* under different N nutrition conditions. **A.** Representative GS western blot of total soluble proteins (8.5 µg per lane) extracted from the roots and aerial parts of control and treated seedlings after 3 and 24 hours. Duplicates are shown side by side for each condition. **B.** and **C.** GS activity measured by the transferase reaction after 3h and 24h of treatment, respectively. Results are shown as mean ± SD of three independent pools of 3 or 4 seedlings, except when marked with † (in which case, n=2).

After 24 hours the above described pattern is no longer seen and there is increasing variation between duplicates. Noteworthy are the higher amounts of GS1 present in leaves in response to higher concentrations of either substrate, when compared to control and lower N concentrations. In terms of activity, there is a higher variability within each group tested, yet the activity is higher than the one registered at 3 hours. Roots seem to show a slight decrease

in response to NH_4^+ treatment, which is not in agreement with the western blot, where GS contents seem higher under these conditions than in the untreated control. In the aerial organs, an increase in activity was seen only when seedlings were treated with 10 mM NO_3^-, which is in accordance with the data of the western blot. Nevertheless, these are preliminary results that should be interpreted with caution and that require confirmation by testing additional samples.

Taken together, these data do not describe a clear mechanism of GS regulation in function of N treatment. Variations were indeed seen, most patently at the protein level, both quantity and activity-wise, yet the RNA, protein and activity levels do not correlate, which could account for the action of modulatory mechanisms occurring before and after transcription and also posttranslationally. Considering the complex nature of the GS gene family and its known regulatory mechanisms, such a possibility is not to be discarded.

3.6. Construction of a RNA interference vector for the knock-down of *MtNLP7*

In order to assay the function of *MtNLP7* in the context of the rhizobium symbiosis, and RNA interference approach was initiated. RNA interference is a powerful tool to study gene function for it allows the knock-down of a specific gene, through a relatively simple procedure. Nevertheless, it is not without limitations, namely the fact that complete abrogation of expression is seldom seen and the low level of expression may be sufficient to grant a normal phenotype.

The strategy employed in this work is based upon the expression of a 185 bp perfect inverted repeat of a specific sequence of the *MtNLP7* gene separated by a spacer of 389 bp. This sequence, when transcribed, will lead to the formation of double-stranded RNA (dsRNA) via the hybridization of the *MtNLP7* sequence, with the formation of a hairpin (Figure 3.6.1). This secondary structure is amicable to recognition by the ribonuclease III enzyme Dicer, which cleaves the dsRNA into small interfering RNAs (siRNAs) of 25 nucleotides (Hamilton and Baulcombe, 1999), allowing the formation of the RISC complex (RNA-induced Silencing Complex). This complex then recognises the mRNA complementary to the siRNAs and elicits its degradation (Nykanen *et al.*, 2001). Considering that the 185 bp sequence is predicted to be unique to the *MtNLP7* gene (as assayed using NCBI's BLAST algorithm against the *M.*

truncatula genome (Altschul *et al.*, 1997)), only the expression of this gene should be abrogated.

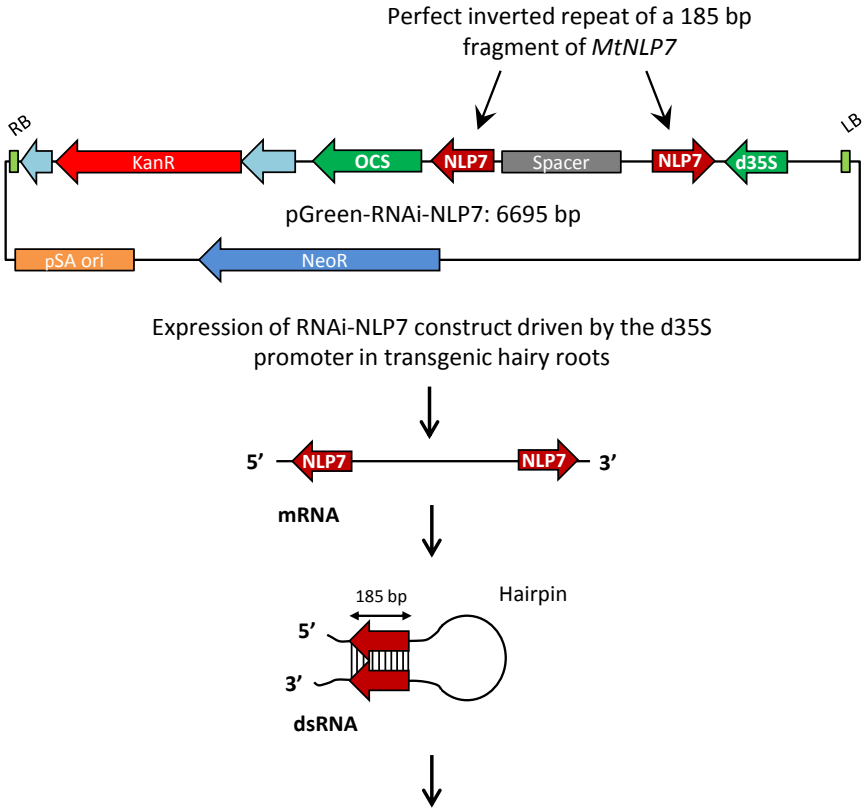

Figure 3.6.1. RNAi strategy for the knock-down of the *MtNLP7* gene. Expression from the d35S promoter in the pGreen-RNAi-NLP7 leads to the formation of mRNA that contains at each end a 185 bp sequence of the *MtNLP7* gene in opposite orientations, in such a way that these sequences can hybridise and form dsRNA with a hairpin. This structure is recognised by Dicer, cleaved into siRNAs with the formation of the RISC complex, which will promote the degradation of *MtNLP7* mRNA and lead to the knock-down of the expression of this gene.

The pGreen-RNAi-NLP7 was constructed as described in Chapter 2.7, introduced in *Agrobacterium rhizogenes* and seedlings were transformed with *A. rhizogenes* for the generation of transgenic hairy roots with reduced expression of *MtNLP7*, under kanamycin selection to inhibit growth of nontransformed adventitious laterals. Control plants subjected to sectioning of the root tip but that were not inoculated with *A. rhizogenes* were also grown in the presence and absence of kanamycin. In Figure 3.6.2, root and shoot development of control and inoculated plants, growing either in the absence or presence of kanamycin, are compared. It can be observed that kanamycin positively selects for transformed plants, as seen

by the fact that root does not develop in control plants in the presence of kanamycin (Figure 3.6.2 A and B). However, in the case of plants inoculated with *A. rhizogenes*, growth is allowed in the presence of the antibiotic and hairy roots are formed, which have a distinct physiology than control plants with normal development (Figure 3.6.2 A and C).

Results regarding the success of the RNAi strategy and possible effects of the abrogation of the expression of *MtNLP7* are, at this moment, pending.

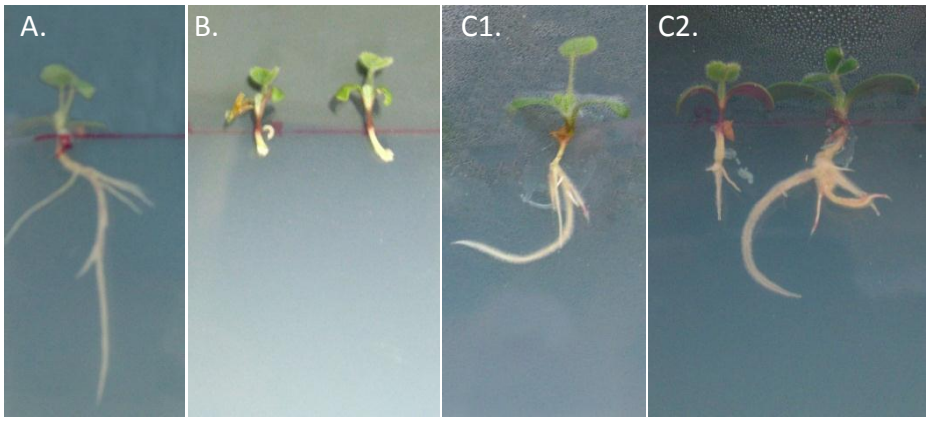

Figure 3.6.2. Production of *Medicago truncatula* transgenic hairy roots. **A.** Control plantlet (sectioned but not inoculated) grown in the absence of kanamycin. **B.** Control plantlets (sectioned but not inoculated) grown on medium containing 25 $mg \cdot L^{-1}$ of kanamycin. **C1-C2.** *A. rhizogenes*-inoculated plantlets with transformed hairy roots grown on medium containing 25 $mg \cdot L^{-1}$ of kanamycin.

Chapter IV

Discussion

The interaction of plants with the surrounding environment is an intricate and intimate one. Their response to environmental cues is obvious at the physiological level, yet from a molecular point of view much is yet to be described. In this work, three novel genes of the model legume *Medicago truncatula* began to be evaluated, namely *MtAMT3*, *MtNR3* and *MtNLP7*, with a particular focus in their response to the nitrogen environment to which they were subjected. The study of the response to environmental cues was extended to the glutamine synthetase gene family, given the central role of these enzymes in N metabolism.

4.1. *MtAMT3*: gene family and potential function

MtAMT3 is a member of the AMT2 family of ammonium transporters (Figure 3.2.3). This is, to our knowledge, the first study that focuses on this particular gene and in members of this family of ammonium transporters in *M. truncatula*. The AMT2 family of ammonium transporters is closer in sequence identity to their prokaryotic homologues than to members of the AMT1 family within the same species (Figure 3.2.3), yet they too are high-affinity NH_4^+ transporters (Sohlenkamp *et al.*, 2000; Sohlenkamp *et al.*, 2002; Simon-Rosin *et al.*, 2003). Whether these transporters play a unique function in N metabolism has not been fully elucidated, but the fact that they are subjected to differential expression within the plant is indicative that they are under different regulatory mechanisms and therefore may play specific roles in the plant physiology. In fact, it has been suggested that these transporters could be involved in the recovery of ammonium lost from plant cells during photorespiration in organs such as shoots and leaves (Sohlenkamp *et al.*, 2000), yet a posterior RNAi study did not reveal a significant phenotype, thus excluding an essential role of AMT2 during photorespiration in *A. thaliana* (Sohlenkamp *et al.*, 2002). In *L. japonicus*, a particular role in the recovery of

ammonium that is lost from nodule cells to the apoplast was proposed (Simon-Rosin *et al.*, 2003), but, until this moment, this hypothesis has not yet been proven. In the particular case of *MtAMT3*, it is interesting to note that its expression, under normal conditions, is circumscribed to the root and nodules (Figure 3.1.1). A second member of the AMT2 family was identified, which, despite having a different sequence, is also annotated in the public databases as *MtAMT3*. Comparing with the gene under study, this second *MtAMT3* has a more global expression profile (Figure 3.2.4). These two genes share 70% of amino acid sequence identity (Figure 3.2.3), yet considering the difference in their expression patterns, one can hypothesise that they play non-overlapping roles and that the root/nodule-specific *MtAMT3* exerts a distinct physiological role, specific to this particular and specialized organ. Indeed, an ammonium transporter is likely required in the symbiosome membrane of infected cells, so that transport of the NH_4^+ produced by N_2-fixing bacteria can reach the plant cytosol, a paramount exchange in this symbiotic model. However, until this moment, the molecular identity of this transporter remains to be elucidated. The root/nodule-specific expression of *MtAMT3* thus stimulates the hypothesis that this could be such a transporter.

In this work, a differential expression of *MtAMT3* was seen in two distinct contexts of the plant-rhizobium symbiosis, namely the inoculation with the *fixJ Sinorhizobium* mutant and treatment with nitrate after the establishment of a successful symbiosis with a wild-type *Sinorhizobium* strain (Figure 3.3.2). Despite the fact that in both cases N_2 fixation is impaired and nodule senescence occurs, in the former the plant has no available N source, while in the latter nodule senescence occurs due to the fact that it is more advantageous for the plant to reduce nitrate than to support the energetically expensive bacteria-mediated N_2 fixation and, for this reason, a differential transcription reprogramming is seen in either case (Moreau *et al.*, 2011). In this context, upregulation of *MtAMT3* in the Fix^- situation and downregulation when nitrate is provided fits the possibility of *MtAMT3* being involved in the transport of bacterially-produced NH_4^+ to the plant cytosol. In the first case, the plant would be responding to an appalling lack of nitrogen, thus trying to recover whatever little ammonium is released from the bacteria. In the second case, the plant is plentifully supplied in terms of NH_4^+ and therefore needs not the activity of a nodule-specific ammonium transporter. A similar downregulation was reported by the *Mt*GEA data, as shown in Figure 3.1.1. This correlates with the PPT-sustained downregulation of this same gene, for GS inhibition leads to the accumulation of its substrate, NH_4^+. Interestingly, in *A. thaliana*, a feedback inhibition mechanism of *AtAMT1;1* was recently described. Increasing external concentrations of NH_4^+ correlated with decreased ammonium uptake and with increasing levels of phosphorylated AtAMT1;1 at T460, a threonine that had been previously shown to be essential for the functionality of the

transporter in a site-directed mutagenesis study (Loqué *et al.*, 2007; Lanquar *et al.*, 2009). Even though this refers to a posttranslational regulatory mechanism and what was observed in this study were differences in terms of transcript amount, it is nonetheless interesting to consider the idea that the expression of *MtAMT3* can be negatively regulated by the substrate it carries, ammonium. Finally, the seedlings nutrition experiment showed that *MtAMT3* is not expressed in the aerial organs (Figure 3.4.1 A), which is in accordance with the transcriptional data already available. Interestingly, *MtAMT3* appears to be negatively regulated by NO_3^-, as observed in nodules (Figure 3.3.2), but whether this is a direct effect of NO_3^- or an indirect consequence of increased intercellular levels of NH_4^+ originating from nitrate reduction is not known and further studies are required to understand this regulatory mechanism.

4.2. *MtNR3* and possible roles in the legume-rhizobium symbiosis

Regarding *MtNR3*, it was found that it encodes a protein with domains typical of nitrate reductases (Figure 3.2.5) and also that it appears to be nodule-specific (Figure 3.1.1), which is intriguing, given that in nodules nitrate is not a N source. Its function, therefore, might serve a different purpose other than providing the substrate for N assimilation. Considering that a role in NO production has been ascribed to this family of enzymes and how NO signalling is related to nodule development and metabolism, simultaneously being required for the establishment of successful symbiosis, yet inhibiting N_2 fixation, the particular expression profile of *MtNR3* further proposes the connection between NR function, NO production and nodule development.

In this work, it was shown that expression of *MtNR3* is decreased in NO_3^--treated nodules, fact that correlates with the *Mt*GEA data (Figure 3.3.2). As mentioned previously, a role for NR was proposed in the maintenance of the energy status required for N_2 fixation, via a NO_3^--NO respiration process in nodules. In NO_3^--treated nodules this process is no longer required, fact that could account for the downregulation of this transcript. Similarly, it was interesting to verify that *MtNR3* was upregulated when the symbiosis was established with a better N_2-fixing symbiont than *S. meliloti*, *S. medicae*. Perhaps this increase in N_2 fixation, which implies higher energy demands, can be achieved through the NO_3^--NO respiration process proposed by Horchani *et al*. (2011).

Expression of *MtNR3* was also increased in Fix^- nodules. In these particular conditions, GS was found to be inactivated by NO (Melo *et al.*, 2011), which could imply an increased NO

production in Fix$^-$ nodules. If MtNR3 is indeed a NO producing enzyme, its upregulation in Fix$^-$ nodules correlates with increased NO levels. *MtNR3* was also found to be upregulated in nodulating split roots with limited N_2 availability, as described in the *Mt*GEA data, a condition which is similar to the Fix$^-$ model (nodulation occurs, yet fixation is impaired). Nonetheless, NR is a tightly regulated enzyme and these hypotheses are still notional ideas that serve as stimuli for future discussion and research.

4.3. *MtNLP7* is a putative transcription factor central in N metabolism

Given the current knowledge of *MtNLP7* homologues in *A. thaliana* and *C. reinhardtii*, this gene appears to be a central regulator of N metabolism in plants, as connections have been established between this gene and the metabolism of ammonium and nitrate. In legumes, however, specifically in a N_2 fixation symbiotic model, this is the first work that focuses on this gene and tries to establish its function and regulation.

Previously, a role as a transcription factor had been proposed for NLP7, with strong evidence pointing in that direction. Bioinformatic analysis of the amino acid sequence of the homologue in *M*. *truncatula* showed that this protein contains domains typical of transcription factors, namely a RWP-RK DNA-binding domain, a PB1 homo/heterodimerization domain, a nuclear export signal and GAF domains, which bind small molecules such as cGMP, cAMP and NO (Figure 3.2.6). The GAF domains, acting as sensors, possibly control the exposure of the nuclear export signal and thus regulate the commute between cytosol and nucleus, serving as an on/off switch that rules the activity of MtNLP7 as a transcription factor. In this context, the possibility of NO binding to the GAF domain further highlights the importance of NO as a signalling molecule and its involvement in N metabolism.

In terms of responses to environmental cues, *MtNLP7* is upregulated both in Fix$^-$ and in nitrate-treated nodules, which agrees with the transcriptomic data provided by the *Mt*GEA (Figure 3.3.2). The upregulation of *MtNLP7* in Fix$^-$ nodules is in agreement with what has been previously described for *CrNIT2*, namely ammonium-mediated repression, given that under these experimental conditions the amounts of NH_4^+ decrease due to inhibition of N_2 fixation. In NH_4^+-treated seedlings, a similar downregulation was observed in roots after 3 hours. Conversely, after 24 hours of treatment, upregulation of this transcript was detected both in roots and the aerial organs (Figure 3.4.1 B). *MtNLP7* has also been described to be upregulated in response to increasing periods of PPT-treatment, which, as previously mentioned,

theoretically leads to the accumulation of the substrate for GS, NH_4^+. These contrasting effects could possibly be explained by variations in the equilibrium between the extra- and intracellular concentrations of NH_4^+, which are likely to be different in each of the experimental set-ups tested, yet such conclusions cannot be drawn for these data.

In *C. reinhardtii*, nitrate did not induce *CrNit2* expression, but it was required for Nit2 binding of the *CrNIA1* promoter (Camargo *et al.*, 2007). In higher plants, however, apart from transcriptomic studies, the expression of *NLP7* to distinct N sources has not been studied to date. This work showed that *MtNLP7* is upregulated in nodules and in roots of seedlings in response to NO_3^-. Interestingly, in seedlings after 3 hours of treatment, the expression of *MtNLP7* seems to be repressed by low NO_3^- concentrations, whilst the response to higher concentrations is the opposite. High- and low-affinity transporters are responsible for nitrate uptake in plants (Tsay *et al.*, 2007), and this differential response to high and low concentrations of NO_3^- could be due to the activation of distinct signal transduction pathways activated by each type of transporter.

4.4. GS responses to environmental cues

The key position exerted by GS in N metabolism stresses the necessity of a fine description of the main regulatory mechanisms that control these enzymes, a description that cannot ignore a careful screening for responses to environmental cues, specifically, inorganic nitrogen. In this work, the effects of treatment with different concentrations of NO_3^- and NH_4^+ in three-week old seedlings of *M. truncatula* grown in N-starvation were evaluated, both at the RNA and protein levels, at two distinct time points (Figures 3.5.1 and 3.5.2). A clear response, reflected in terms of RNA and protein levels and in agreement with GS activity, was not seen in any of the conditions tested. Nevertheless, interesting responses were observed, especially at the protein level, and differences detected between RNA and protein quantities and activity levels may be accounted by regulatory mechanisms acting before and after transcription and posttranscriptionally as well.

At the RNA level significant differences were not observed. In terms of protein quantity and activity, an interesting variation was found in roots 3 hours after the start of treatment. Higher amounts of GS, most prominently GS2, were found in seedlings treated with 10 mM NO_3^- and 10 mM NH_4^+, while smaller amounts of protein were detected when the same substrates were provided at submillimolar concentrations. Similarly to the case of *MtNLP7*, this

could be the end result of the activation of distinct signal transduction pathways due to the activation of either high- or low-affinity transporters.

It was also clear that the response of GS varies significantly after 3 or 24 hours of treatment. This variation is not surprising and confirms that if one is looking for adaptive responses to changes in the environment, these can be found as soon as 3 hours after this change occurs and that after 24 hours similar responses are no longer observed. In fact, a study in *M. sativa* found an increase in the RNA amount of *MsGS2* as soon as 0.5 hours after treatment with 10 mM NO_3^-, with a maximum response after 1.5 hours. By 24 hours of treatment, these values had returned to the ones initially found (Zozaya-Hinchliffe *et al.*, 2005).

In conclusion, it is still not possible to infer a clear response of a GS gene to any of the conditions tested or its significance from a physiological point of view. Nevertheless, interesting variations were observed, which entice further research. It could be the case that GS is globally irresponsive to these changes and that adaptive responses occur upstream of the assimilatory reaction that it catalyses. From this perspective, a similarly independent response is not expected if, besides an N nutrient, the environmental status in terms of carbon is changed, considering that carbon and nitrogen metabolism are linked through the GS/GOGAT cycle. Previous work has shown just that in *M. sativa*, in which the response to a combination of sucrose and NO_3^- was far greater than when either metabolite was supplied independently (Zozaya-Hinchliffe *et al.*, 2005). Considering the complex nature of the GS gene family, its known regulatory mechanisms and its central role in the metabolism of nitrogen and, consequently, in the plant's nutrition, development and yield, the characterization of its regulation by environmental cues is a vital necessity and could suggest new and improved agricultural practises.

Chapter V

Conclusion

The metabolism of nitrogen in the context of the legume-rhizobium symbiosis provided the background against which this work was developed, which aimed at analysing the potential of putative N sensors and regulators and their response, along with that of central genes of N metabolism, to environmental cues. In this regard, this work provides evidence for the potential of *MtAMT3*, *MtNR3* and *MtNLP7* as modulators of the N status within the cell and shows their response and that of the GS gene family to differential N provision.

First, a focus on the bioinformatics data available provided valuable information regarding this set of previously unknown genes. The analysis of their transcription profile showed that the expression of *MtAMT3* is limited to roots and nodules and that the expression of *MtNR3* is even more restrained, as it is present only in nodules. Analysing the amino acid sequence of MtAMT3 and MtNR3 showed that the first is a member of the AMT2 family of ammonium transporters and that the latter has the typical structure of a nitrate reductase. A similar analysis for MtNLP7 showed that this might be a transcription factor controlled through binding of small molecules in GAF domains.

Secondly, the expression-wise variation of *MtAMT3*, *MtNR3* and *MtNLP7* in root nodules under different conditions was quantified by RT-qPCR. It is shown that all three genes are overexpressed in ineffective *fixJ* (Fix^-) nodules and that a two-day treatment with nitrate led to the downregulation *MtAMT3* and *MtNR3*, but not of *MtNLP7*. Additionally, the establishment of symbiosis with *S. medicae*, a better nitrogen fixer than *S. meliloti*, did not significantly alter the expression of *MtAMT3* and *MtNLP7*, yet it led to the increase in the mRNA levels of *MtNR3*. These observations, in the context of nodule metabolism, stimulate the hypotheses that *MtAMT3* might be the currently unidentified symbiotic ammonium transporter and that *MtNR3* is involved in a NO_3^--NO respiration process and/or in the production of nitric oxide.

In seedlings, the expression of *MtAMT3* was restricted to roots and seemed to be inhibited by nitrate. In the case of *MtNLP7*, distinct expression patterns were observed at

either time point analysed, being induced by high nitrate concentrations and repressed by ammonium at 3 hours, yet induced by ammonium at 24 hours. The role of *MtNLP7* is yet to be fully characterized, but the variations observed place it as having a central role in the metabolism of nitrogen.

The simple and versatile experimental set-up using three-week old seedlings allowed also the screening of responses of GS genes to different N treatments, at the levels of RNA, protein and activity. However, these results are still inconclusive and a clear response was not evident.

Together, these data point to different roles played by these proteins in the regulation of N metabolism in the symbiotic relationship between *M. truncatula* and *Sinorhizobium* and entice a deeper characterization of their function. The view of the role that nutrients play in plants has evolved from these being seen as simple building blocks to recognition as potential signalling molecules and this and similar studies provide novel insights as to how plants curb growth, development and activity in response to fluctuating environmental conditions.

Chapter VI

Future perspectives

Future studies beg the cloning of the *MtAMT3*, *MtNR3* and *MtNLP7* gene sequences. This is an essential step to perform several experiments that will further look into the function of these genes. This includes the full characterization of the cDNA, including the characterization of the 3' and 5´ untranslated regions (UTRs). The possession of this information and of the cloned sequences allows the execution of important experiments that would enable the identification of both sub-cellular and morphological location of these proteins. Additionally, it would permit the production of recombinant proteins in *E. coli*, a simple system for obtaining high yields of protein. This capacity would enable a variety of studies necessary to clarify their function and that are only possible with purified protein.

Through the cloning of GFP (Green Fluorescent Protein) fusion proteins, which could then be produced in *E. coli*, transformed in protoplasts of heterologous systems such as *Nicotiana tabacum* and *A. thaliana* and then visualised by confocal fluorescence microscopy, it would be possible to see whether these proteins localise in the nucleus, in the cytoplasmic membrane or in a specific organelle within the cell. This is of particular interest in the case of MtAMT3, for it would confirm whether this is indeed a transmembrane protein, and in the case of MtNLP7, given that its localization in the nucleus would provide further evidence to its role as a transcription factor.

Moreover, the production of *in situ* hybridisation probes specific to these genes would be useful to determine the morphological location of these mRNAs, namely in the complex anatomy of the root nodule. Considering *MtNR3*, this type of analysis in a time course study of root nodule development, coupled with quantitative PCR, would help to establish whether this particular nitrate reductase plays a significant role in nodule development, since it is possibly involved in NO production, which has a positive effect in the establishment of the symbiosis (del Giudice *et al.*, 2011). Additionally, it is important to validate the *MtGEA* data and analyse the expression of *MtNR3* in all organs of the plant.

Upon production of recombinant MtAMT3 in *E. coli*, a variety of enzymatic tests could be performed, such as the identification of its de facto substrate, kinetics and susceptibility to different pH values in the medium. To determine the functionality of MtAMT3 as an ammonium transporter, a first and classic experiment to perform is a complementation assay in the *S. cerevisiae* strain MLY131a/α. This strain is defective in all three endogenous ammonium transporters (Δ*mep1*, Δ*mep2*, Δ*mep3*) and, therefore, is unable to grow on medium containing less than 5 mM ammonium as sole nitrogen source (Lorenz and Heitman, 1998). This is a relatively simple system to study the characteristics of this transporter and the conditions of the experiment can be easily manipulated by changing the medium in which the yeast is growing.

Regarding MtNR3, the purification of the protein would allow the characterization of its enzymatic activity, namely the verification that it is indeed able to produce NO, both *in vitro* and *in vivo*.

As for MtNLP7, gel shift assays would further confirm whether this protein is a transcription factor, and, what is more, which are the target genes it activates. Of particular interest would be testing the promoters of the nitrate reductases of *M. truncatula* and verify whether they are controlled by MtNLP7, given that it has been shown that the Nit2 protein of *C. reinhardtii* binds the *NIA1* promoter (Camargo *et al.*, 2007). Other genes could be tested, including those of GS1 and GS2, and those of the AMT family. In *C. reinhardtii* it was shown that Nit2 downregulates the expression of *CrAMT1;1* (Gonzalez-Ballester *et al.*, 2004) and a similar role could be played by NLP7 in *M. truncatula*, thus aiding in the decoding of this signalling pathway. Moreover, and in an effort to understand not only which genes *MtNLP7* regulates but also how it is regulated itself, it would be valuable to learn exactly what binds the GAF domains of NLP7 in *M. truncatula* and whether this regulates translocation to and from the nucleus.

The study of the function of *MtNLP7* through RNAi, initiated in this work, should be continued further. A possible phenotypic change would be the overexpression of genes belonging to the AMT family and therefore RT-qPCR should be performed to confirm this hypothesis. To counter the drawbacks of RNAi, homozygous knock-out mutants for *MtNLP7* should be attained and their phenotype studied further. While similar work has been done in *A. thaliana*, this particular gene has not yet been studied in a legume plant, and given its apparent central role in the regulation of N metabolism, its study in the model legume *M. truncatula* is of outstanding interest, when the particularities and importance of the N_2-fixing symbiosis are considered.

Given the practicality of the seedling system described in this work, similar experiments could be performed to assay the response of GS genes to a class of metabolites, including carbon skeletons, such as sucrose, amino acids such as glutamine, and combinations of these molecules with N metabolites, such as nitrate or ammonium.

The set of proposed experiments described in the previous paragraphs would undoubtedly provide new and important clues that would help in the decoding of the signalling pathways in the metabolism of nitrogen in *Medicago truncatula* and, given its role as a model system, in legume plants in general.

References

World Population Prospects: The 2010 Revision, 2011. Department of Economic and Social Affairs - Population Division, New York.

Altschul, S. F., Madden, T. L*., et al.* (1997). *Gapped BLAST and PSI-BLAST: a new generation of protein database search programs*. Nucleic Acids Res, **25**(17): 3389-3402.

Aravind, L. and Ponting, C. P. (1997). *The GAF domain: an evolutionary link between diverse phototransducing proteins*. Trends in Biochemical Sciences, **22**(12): 458-459.

Ayling, S. M. (1993). *The effect of ammonium ions on membrane potential and anion flux in roots of barley and tomato*. Plant, Cell & Environment, **16**(3): 297-303.

Baier, R., Schiene, K*., et al.* (1999). *Alfalfa and tobacco cells react differently to chitin oligosaccharides and sinorhizobium meliloti nodulation factors*. Planta, **210**(1): 157-164.

Baudouin, E., Pieuchot, L*., et al.* (2006). *Nitric Oxide Is Formed in Medicago truncatula-Sinorhizobium meliloti Functional Nodules*. Molecular Plant-Microbe Interactions, **19**(9): 970-975.

Beever, D., Brentrup, F*., et al.* (2007). *Sustainable Management of the Nitrogen Cycle in Agriculture and Mitigation of Reactive Nitrogen Side Effects*. International Fertilizer Industry Association.

Benedito, V. A., Torres-Jerez, I*., et al.* (2008). *A gene expression atlas of the model legume Medicago truncatula*. Plant J, **55**(3): 504-513.

Benson, D. A., Karsch-Mizrachi, I*., et al.* (2012). *GenBank*. Nucleic Acids Res, **40**(Database issue): D48-53.

Bernard, S. M. and Habash, D. Z. (2009). *The importance of cytosolic glutamine synthetase in nitrogen assimilation and recycling*. New Phytologist, **182**(3): 608-620.

Bradford, M. M. (1976). *A rapid and sensitive method for the quantitation of microgram quantities of protein utilizing the principle of protein-dye binding*. Anal Biochem, **72**: 248-254.

Braun, E. (2007). *Reactive Nitrogen in the Environment: Too Much or Too Little of a Good Thing*. United Nations Environmental Programme.

Camargo, A., Llamas, A.*, et al.* (2007). *Nitrate signaling by the regulatory gene NIT2 in Chlamydomonas*. Plant Cell, **19**(11): 3491-3503.

Campbell, W. H. (1999). *Nitrate Reductase Structure, Function and Regulation: Bridging the Gap between Biochemistry and Physiology*. Annu Rev Plant Physiol Plant Mol Biol, **50**: 277-303.

Cannon, S. B., May, G. D.*, et al.* (2009). *Three sequenced legume genomes and many crop species: rich opportunities for translational genomics*. Plant Physiol, **151**(3): 970-977.

Carvalho, H., Sunkel, C.*, et al.* (1997). *Heteromeric assembly of the cytosolic glutamine synthetase polypeptides of Medicago truncatula: complementation of a glnA Escherichia coli mutant with a plant domain-swapped enzyme*. Plant Mol Biol, **35**(5): 623-632.

Castaings, L., Camargo, A.*, et al.* (2009). *The nodule inception-like protein 7 modulates nitrate sensing and metabolism in Arabidopsis*. Plant J, **57**(3): 426-435.

Charpentier, M. and Oldroyd, G. (2010). *How close are we to nitrogen-fixing cereals?* Curr Opin Plant Biol, **13**(5): 556-564.

Cook, D. R. (1999). *Medicago truncatula - a model in the making!* Curr Opin Plant Biol, **2**(4): 301-304.

Cueto, M., Hernandez-Perera, O.*, et al.* (1996). *Presence of nitric oxide synthase activity in roots and nodules of Lupinus albus*. FEBS Letters, **398**(2-3): 159-164.

Cullimore, J. and Miflin, B. (1984). *Immunological Studies on Glutamine Synthetase using Antisera Raised to the Two Plant Forms of the Enzyme from Phaseolus Root Nodules*. Journal of Experimental Botany, **35**(4): 581-587.

Cullimore, J. V. and Sims, A. P. (1980). *An association between photorespiration and protein catabolism: Studies with Chlamydomonas*. Planta, **150**(5): 392-396.

Czechowski, T., Stitt, M.*, et al.* (2005). *Genome-wide identification and testing of superior reference genes for transcript normalization in Arabidopsis*. Plant Physiol, **139**(1): 5-17.

D'Autreaux, B., Tucker, N. P.*, et al.* (2005). *A non-haem iron centre in the transcription factor NorR senses nitric oxide*. Nature, **437**(7059): 769-772.

Day, D. A., Poole, P. S.*, et al.* (2001). *Ammonia and amino acid transport across symbiotic membranes in nitrogen-fixing legume nodules*. Cellular and Molecular Life Sciences, **58**(1): 61-71.

Dean, J. V. and Harper, J. E. (1988). *The Conversion of Nitrite to Nitrogen Oxide(s) by the Constitutive NAD(P)H-Nitrate Reductase Enzyme from Soybean*. Plant Physiol, **88**(2): 389-395.

del Giudice, J., Cam, Y.*, et al.* (2011). *Nitric oxide is required for an optimal establishment of the Medicago truncatula–Sinorhizobium meliloti symbiosis*. New Phytologist, **191**(2): 405-417.

del Río, L. A., Javier Corpas, F.*, et al.* (2004). *Nitric oxide and nitric oxide synthase activity in plants*. Phytochemistry, **65**(7): 783-792.

Delledonne, M. (2005). *NO news is good news for plants*. Curr Opin Plant Biol, **8**(4): 390-396.

Erisman, J. W., Sutton, M. A.*, et al.* (2008). *How a century of ammonia synthesis changed the world*. Nature Geosci, **1**(10): 636-639.

Ferrarini, A., De Stefano, M.*, et al.* (2008). *Expression of Medicago truncatula Genes Responsive to Nitric Oxide in Pathogenic and Symbiotic Conditions*. Molecular Plant-Microbe Interactions, **21**(6): 781-790.

Forde, B. G. and Lea, P. J. (2007). *Glutamate in plants: metabolism, regulation, and signalling*. Journal of Experimental Botany, **58**(9): 2339-2358.

Foresi, N., Correa-Aragunde, N.*, et al.* (2010). *Characterization of a nitric oxide synthase from the plant kingdom: NO generation from the green alga Ostreococcus tauri is light irradiance and growth phase dependent*. Plant Cell, **22**(11): 3816-3830.

Fournier, J., Timmers, A. C.*, et al.* (2008). *Mechanism of infection thread elongation in root hairs of Medicago truncatula and dynamic interplay with associated rhizobial colonization*. Plant Physiol, **148**(4): 1985-1995.

Fried, M., Zsoldos, F.*, et al.* (1965). *Characterizing the NO_3 and NH_4 Uptake Process of Rice Roots by Use of ^{15}N Labelled NH_4NO_3*. Physiologia Plantarum, **18**(2): 313-320.

Gazzarrini, S., Lejay, L.*, et al.* (1999). *Three functional transporters for constitutive, diurnally regulated, and starvation-induced uptake of ammonium into Arabidopsis roots*. Plant Cell, **11**(5): 937-948.

Gomez, S. K., Javot, H.*, et al.* (2009). *Medicago truncatula and Glomus intraradices gene expression in cortical cells harboring arbuscules in the arbuscular mycorrhizal symbiosis*. BMC Plant Biol, **9**: 10.

Gonzalez-Ballester, D., Camargo, A.*, et al.* (2004). *Ammonium transporter genes in Chlamydomonas: the nitrate-specific regulatory gene Nit2 is involved in Amt1;1 expression*. Plant Mol Biol, **56**(6): 863-878.

Gould, K. S., Lamotte, O.*, et al.* (2003). *Nitric oxide production in tobacco leaf cells: a generalized stress response?* Plant, Cell & Environment, **26**(11): 1851-1862.

Graham, P. H. and Vance, C. P. (2003). *Legumes: importance and constraints to greater use*. Plant Physiol, **131**(3): 872-877.

Greenwood, D. (1982). *Nitrogen supply and crop yield: The global scene*. Plant and Soil, **67**(1): 45-59.

Hakoyama, T., Niimi, K.*, et al.* (2009). *Host plant genome overcomes the lack of a bacterial gene for symbiotic nitrogen fixation*. Nature, **462**(7272): 514-517.

Hamilton, A. J. and Baulcombe, D. C. (1999). *A Species of Small Antisense RNA in Posttranscriptional Gene Silencing in Plants*. Science, **286**(5441): 950-952.

He, J., Benedito, V. A.*, et al.* (2009). *The Medicago truncatula gene expression atlas web server*. BMC Bioinformatics, **10**: 441.

Heidstra, R. and Bisseling, T. (1996). *Nod factor-induced host responses and mechanisms of Nod factor perception*. New Phytologist, **133**(1): 25-43.

Hellens, R. P., Edwards, E. A.*, et al.* (2000). *pGreen: a versatile and flexible binary Ti vector for Agrobacterium-mediated plant transformation*. Plant Molecular biology, **42**(6): 819-832.

Hirel, B., Bouet, C.*, et al.* (1987). *Glutamine synthetase genes are regulated by ammonia provided externally or by symbiotic nitrogen fixation*. EMBO J, **6**(5): 1167-1171.

Hirsch, A. M. and Fang, Y. (1994). *Plant hormones and nodulation: what's the connection?* Plant Mol Biol, **26**(1): 5-9.

Ho, Y.-S. J., Burden, L. M.*, et al.* (2000). *Structure of the GAF domain, a ubiquitous signaling motif and a new class of cyclic GMP receptor*. EMBO J, **19**(20): 5288-5299.

Horchani, F., Prevot, M.*, et al.* (2011). *Both plant and bacterial nitrate reductases contribute to nitric oxide production in Medicago truncatula nitrogen-fixing nodules*. Plant Physiol, **155**(2): 1023-1036.

Irwin, N. and Janssen, K. (2001). *Vectors and bacterial strains*. Molecular Cloning: A Laboratory Manual. J Sambrook and David W. Russell. New York, Cold Spring Harbor Laboratory Press. **III:** A3.6.

Ishiyama, K., Inoue, E.*, et al.* (2004). *Biochemical Background and Compartmentalized Functions of Cytosolic Glutamine Synthetase for Active Ammonium Assimilation in Rice Roots*. Plant and Cell Physiology, **45**(11): 1640-1647.

Ishiyama, K., Inoue, E.*, et al.* (2004). *Kinetic Properties and Ammonium-dependent Regulation of Cytosolic Isoenzymes of Glutamine Synthetase in Arabidopsis*. Journal of Biological Chemistry, **279**(16): 16598-16605.

Jaffe, A., Ogura, T.*, et al.* (1985). *Effects of the ccd function of the F plasmid on bacterial growth*. J Bacteriol, **163**(3): 841-849.

Jain, M., Nijhawan, A.*, et al.* (2006). *Validation of housekeeping genes as internal control for studying gene expression in rice by quantitative real-time PCR*. Biochemical and Biophysical Research Communications, **345**(2): 646-651.

Jones, K. M., Kobayashi, H.*, et al.* (2007). *How rhizobial symbionts invade plants: the Sinorhizobium-Medicago model*. Nat Rev Microbiol, **5**(8): 619-633.

Kanacher, T., Schultz, A.*, et al.* (2002). *A GAF-domain-regulated adenylyl cyclase from Anabaena is a self-activating cAMP switch*. EMBO J, **21**(14): 3672-3680.

Kato, K., Kanahama, K.*, et al.* (2010). *Involvement of nitric oxide in the inhibition of nitrogenase activity by nitrate in Lotus root nodules*. Journal of Plant Physiology, **167**(3): 238-241.

Kraiser, T., Gras, D. E.*, et al.* (2011). *A holistic view of nitrogen acquisition in plants*. J Exp Bot, **62**(4): 1455-1466.

Krogh, A., Larsson, B.*, et al.* (2001). *Predicting transmembrane protein topology with a hidden markov model: application to complete genomes*. Journal of Molecular Biology, **305**(3): 567-580.

Kronzucker, H. J., Siddiqi, M. Y.*, et al.* (1996). *Kinetics of NH_4^+ influx in spruce*. Plant Physiol, **110**(3): 773-779.

la Cour, T., Gupta, R.*, et al.* (2003). *NESbase version 1.0: a database of nuclear export signals*. Nucleic Acids Res, **31**(1): 393-396.

Lam, H. M., Coschigano, K. T.*, et al.* (1996). *The Molecular-Genetics of Nitrogen Assimilation into Amino Acids in Higher Plants*. Annu Rev Plant Physiol Plant Mol Biol, **47**: 569-593.

Lanquar, V., Loque, D.*, et al.* (2009). *Feedback inhibition of ammonium uptake by a phospho-dependent allosteric mechanism in Arabidopsis*. Plant Cell, **21**(11): 3610-3622.

Larkin, M. A., Blackshields, G.*, et al.* (2007). *Clustal W and Clustal X version 2.0*. Bioinformatics, **23**(21): 2947-2948.

Lauter, F. R., Ninnemann, O.*, et al.* (1996). *Preferential expression of an ammonium transporter and of two putative nitrate transporters in root hairs of tomato*. Proc Natl Acad Sci U S A, **93**(15): 8139-8144.

Lea, P. J. and Miflin, B. J. (2010). *Nitrogen Assimilation and its Relevance to Crop Improvement*. Annual Plant Reviews Volume 42, Wiley-Blackwell**:** 1-40.

Letunic, I., Doerks, T.*, et al.* (2012). *SMART 7: recent updates to the protein domain annotation resource*. Nucleic Acids Res, **40**(Database issue): D302-305.

Lima, L., Seabra, A*., et al.* (2006). *Phosphorylation and subsequent interaction with 14-3-3 proteins regulate plastid glutamine synthetase in Medicago truncatula*. Planta, **223**(3): 558-567.

Lima, L., Seabra, A*., et al.* (2006). *Post-translational regulation of cytosolic glutamine synthetase of Medicago truncatula*. Journal of Experimental Botany, **57**(11): 2751-2761.

Limpens, E., Ramos, J*., et al.* (2004). *RNA interference in Agrobacterium rhizogenes-transformed roots of Arabidopsis and Medicago truncatula*. J Exp Bot, **55**(399): 983-992.

Loqué, D., Lalonde, S*., et al.* (2007). *A cytosolic trans-activation domain essential for ammonium uptake*. Nature, **446**(7132): 195-198.

Lorenz, M. C. and Heitman, J. (1998). *The MEP2 ammonium permease regulates pseudohyphal differentiation in Saccharomyces cerevisiae*. EMBO J, **17**(5): 1236-1247.

Lullien, V., Barker, D. G*., et al.* (1987). *Plant gene expression in effective and ineffective root nodules of alfalfa (Medicago sativa)*. Plant Molecular biology, **9**(5): 469-478.

Maki, S., Takiguchi, S*., et al.* (1992). *Modulation of DNA supercoiling activity of Escherichia coli DNA gyrase by F plasmid proteins. Antagonistic actions of LetA (CcdA) and LetD (CcdB) proteins*. J Biol Chem, **267**(17): 12244-12251.

Marquez, A. J., Betti, M*., et al.* (2005). *Nitrate assimilation in Lotus japonicus*. J Exp Bot, **56**(417): 1741-1749.

Marsh, J. F., Rakocevic, A*., et al.* (2007). *Medicago truncatula NIN is essential for rhizobial-independent nodule organogenesis induced by autoactive calcium/calmodulin-dependent protein kinase*. Plant Physiol, **144**(1): 324-335.

Mathesius, U., Charon, C*., et al.* (2000). *Temporal and spatial order of events during the induction of cortical cell divisions in white clover by Rhizobium leguminosarum bv. trifolii inoculation or localized cytokinin addition*. Mol Plant Microbe Interact, **13**(6): 617-628.

Meakin, G. E., Bueno, E*., et al.* (2007). *The contribution of bacteroidal nitrate and nitrite reduction to the formation of nitrosylleghaemoglobin complexes in soybean root nodules*. Microbiology, **153**(Pt 2): 411-419.

Meilhoc, E., Cam, Y*., et al.* (2010). *The response to nitric oxide of the nitrogen-fixing symbiont Sinorhizobium meliloti*. Mol Plant Microbe Interact, **23**(6): 748-759.

Melo, P., Silva, L. S*., et al.* (2011). *Glutamine Synthetase is a Molecular Target of Nitric Oxide in Root Nodules of Medicago truncatula and is regulated by Tyrosine Nitration*. Plant Physiol.

Melo, P. M., Lima, L. g. M.*, et al.* (2003). *Expression of the Plastid-Located Glutamine Synthetase of Medicago truncatula. Accumulation of the Precursor in Root Nodules Reveals an in Vivo Control at the Level of Protein Import into Plastids*. Plant Physiol, **132**(1): 390-399.

Miller, H. I. (2003). *Will we reap what biopharming sows?* Nat Biotech, **21**(5): 480-481.

Minchin, F. R. (1997). *Regulation of oxygen diffusion in legume nodules*. Soil Biology and Biochemistry, **29**(5–6): 881-888.

Moreau, S., Verdenaud, M.*, et al.* (2011). *Transcription reprogramming during root nodule development in Medicago truncatula*. PLoS One, **6**(1): e16463.

Moscat, J., Diaz-Meco, M. T.*, et al.* (2006). *Cell Signaling and Function Organized by PB1 Domain Interactions*. Molecular Cell, **23**(5): 631-640.

Nagata, M., Murakami, E.*, et al.* (2008). *Expression of a class 1 hemoglobin gene and production of nitric oxide in response to symbiotic and pathogenic bacteria in Lotus japonicus*. Mol Plant Microbe Interact, **21**(9): 1175-1183.

Newton, W. E. (2002). *Nitrogen Fixation in Perspective*. Nitrogen Fixation: From Molecules to Crop Productivity. Fabio O. Pedrosa, Mariangela Hungria, Geoffrey Yates and William E. Newton, Springer Netherlands. **38:** 3-8.

Nicot, N., Hausman, J.-F.*, et al.* (2005). *Housekeeping gene selection for real-time RT-PCR normalization in potato during biotic and abiotic stress*. Journal of Experimental Botany, **56**(421): 2907-2914.

Ninnemann, O., Jauniaux, J. C.*, et al.* (1994). *Identification of a high affinity NH_4^+ transporter from plants*. EMBO J, **13**(15): 3464-3471.

Noda, Y., Kohjima, M.*, et al.* (2003). *Molecular Recognition in Dimerization between PB1 Domains*. Journal of Biological Chemistry, **278**(44): 43516-43524.

Nykanen, A., Haley, B.*, et al.* (2001). *ATP requirements and small interfering RNA structure in the RNA interference pathway*. Cell, **107**(3): 309-321.

Oldroyd, G. E. and Downie, J. A. (2004). *Calcium, kinases and nodulation signalling in legumes*. Nat Rev Mol Cell Biol, **5**(7): 566-576.

Oldroyd, G. E. and Downie, J. A. (2008). *Coordinating nodule morphogenesis with rhizobial infection in legumes*. Annu Rev Plant Biol, **59**: 519-546.

Orea, A., Pajuelo, P.*, et al.* (2002). *Isolation of photorespiratory mutants from Lotus japonicus deficient in glutamine synthetase*. Physiologia Plantarum, **115**(3): 352-361.

Ott, T., van Dongen, J. T.*, et al.* (2005). *Symbiotic Leghemoglobins Are Crucial for Nitrogen Fixation in Legume Root Nodules but Not for General Plant Growth and Development*. Current biology : CB, **15**(6): 531-535.

Ovtsyna, A. O., Schultze, M.*, et al.* (2000). *Nod factors of Rhizobium leguminosarum bv. viciae and their fucosylated derivatives stimulate a nod factor cleaving activity in pea roots and are hydrolyzed in vitro by plant chitinases at different rates*. Mol Plant Microbe Interact, **13**(8): 799-807.

Patriarca, E. J., Tate, R.*, et al.* (2004). *Organogenesis of legume root nodules*. Int Rev Cytol, **234**: 201-262.

Paul, M., van Dolleweerd, C.*, et al.* (2011). *Molecular Pharming: future targets and aspirations*. Hum Vaccin, **7**(3): 375-382.

Pfaffl, M. W. (2001). *A new mathematical model for relative quantification in real-time RT-PCR*. Nucleic Acids Res, **29**(9): e45.

Pii, Y., Crimi, M.*, et al.* (2007). *Auxin and nitric oxide control indeterminate nodule formation*. BMC Plant Biol, **7**: 21.

Preisig, O., Zufferey, R.*, et al.* (1996). *A high-affinity cbb3-type cytochrome oxidase terminates the symbiosis-specific respiratory chain of Bradyrhizobium japonicum*. J Bacteriol, **178**(6): 1532-1538.

Prell, J., White, J. P.*, et al.* (2009). *Legumes regulate Rhizobium bacteroid development and persistence by the supply of branched-chain amino acids*. Proc Natl Acad Sci U S A, **106**(30): 12477-12482.

Rockel, P., Strube, F.*, et al.* (2002). *Regulation of nitric oxide (NO) production by plant nitrate reductase in vivo and in vitro*. Journal of Experimental Botany, **53**(366): 103-110.

Rome, S., Brunel, B.*, et al.* (1996). *Evidence that two genomic species of Rhizobium are associated with Medicago truncatula*. Archives of Microbiology, **165**(4): 285-288.

Rome, S., Fernandez, M. P.*, et al.* (1996). *Sinorhizobium medicae sp. nov., Isolated from Annual Medicago spp*. International Journal of Systematic Bacteriology, **46**(4): 972-980.

Rybalkin, S. D., Rybalkina, I. G.*, et al.* (2003). *PDE5 is converted to an activated state upon cGMP binding to the GAF A domain*. EMBO J, **22**(3): 469-478.

Sakihama, Y., Nakamura, S.*, et al.* (2002). *Nitric Oxide Production Mediated by Nitrate Reductase in the Green Alga Chlamydomonas reinhardtii: an Alternative NO Production Pathway in Photosynthetic Organisms*. Plant and Cell Physiology, **43**(3): 290-297.

Sánchez, C., Gates, A. J.*, et al.* (2010). *Production of Nitric Oxide and Nitrosylleghemoglobin Complexes in Soybean Nodules in Response to Flooding*. Molecular Plant-Microbe Interactions, **23**(5): 702-711.

Schauser, L., Roussis, A.*, et al.* (1999). *A plant regulator controlling development of symbiotic root nodules*. Nature, **402**(6758): 191-195.

Schauser, L., Wieloch, W.*, et al.* (2005). *Evolution of NIN-like proteins in Arabidopsis, rice, and Lotus japonicus*. J Mol Evol, **60**(2): 229-237.

Schjoerring, J. K., Husted, S.*, et al.* (2002). *The regulation of ammonium translocation in plants*. Journal of Experimental Botany, **53**(370): 883-890.

Schultz, J., Milpetz, F.*, et al.* (1998). *SMART, a simple modular architecture research tool: identification of signaling domains*. Proc Natl Acad Sci U S A, **95**(11): 5857-5864.

Seabra, A., Vieira, C.*, et al.* (2010). *Medicago truncatula contains a second gene encoding a plastid located glutamine synthetase exclusively expressed in developing seeds*. BMC Plant Biol, **10**(1): 183.

Seabra, A. R., Pereira, P. A.*, et al.* (2012). *Inhibition of Glutamine Synthetase by Phosphinothricin leads to Transcriptome Reprogramming in Root Nodules of Medicago truncatula*. Mol Plant Microbe Interact.

Shelden, M. C., Dong, B.*, et al.* (2001). *Arabidopsis ammonium transporters, AtAMT1;1 and AtAMT1;2, have different biochemical properties and functional roles*. Plant and Soil, **231**(1): 151-160.

Shi, F. M. and Li, Y. Z. (2008). *Verticillium dahliae toxins-induced nitric oxide production in Arabidopsis is major dependent on nitrate reductase*. BMB Rep, **41**(1): 79-85.

Shimoda, Y., Nagata, M.*, et al.* (2005). *Symbiotic rhizobium and nitric oxide induce gene expression of non-symbiotic hemoglobin in Lotus japonicus*. Plant Cell Physiol, **46**(1): 99-107.

Shimoda, Y., Shimoda-Sasakura, F.*, et al.* (2009). *Overexpression of class 1 plant hemoglobin genes enhances symbiotic nitrogen fixation activity between Mesorhizobium loti and Lotus japonicus*. The Plant Journal, **57**(2): 254-263.

Simon-Rosin, U., Wood, C.*, et al.* (2003). *Molecular and cellular characterisation of LjAMT2;1, an ammonium transporter from the model legume Lotus japonicus*. Plant Mol Biol, **51**(1): 99-108.

Smith, B. E. (2002). *Nitrogenase Reveals Its Inner Secrets*. Science, **297**(5587): 1654-1655.

Sohlenkamp, C., Shelden, M.*, et al.* (2000). *Characterization of Arabidopsis AtAMT2, a novel ammonium transporter in plants*. FEBS Letters, **467**(2–3): 273-278.

Sohlenkamp, C., Wood, C. C.*, et al.* (2002). *Characterization of Arabidopsis AtAMT2, a high-affinity ammonium transporter of the plasma membrane*. Plant Physiol, **130**(4): 1788-1796.

Staehelin, C., Granado, J.*, et al.* (1994). *Perception of Rhizobium nodulation factors by tomato cells and inactivation by root chitinases*. Proc Natl Acad Sci U S A, **91**(6): 2196-2200.

Stanford, A. C., Larsen, K.*, et al.* (1993). *Differential expression within the glutamine synthetase gene family of the model legume Medicago truncatula*. Plant Physiol, **103**(1): 73-81.

Tadege, M., Wang, T. L.*, et al.* (2009). *Mutagenesis and beyond! Tools for understanding legume biology*. Plant Physiol, **151**(3): 978-984.

Tadege, M., Wen, J.*, et al.* (2008). *Large-scale insertional mutagenesis using the Tnt1 retrotransposon in the model legume Medicago truncatula*. The Plant Journal, **54**(2): 335-347.

Taiz, L. and Zeiger, E. (2002). *Assimilation of mineral nutrients*. Plant Physiology, Sinauer Associates, Inc., Publishers. **1:** 257-282.

Thomas, G. H., Mullins, J. G. L.*, et al.* (2000). *Membrane topology of the Mep/Amt family of ammonium transporters*. Molecular Microbiology, **37**(2): 331-344.

Tilman, D., Cassman, K. G.*, et al.* (2002). *Agricultural sustainability and intensive production practices*. Nature, **418**(6898): 671-677.

Trieu, A. T., Burleigh, S. H.*, et al.* (2000). *Transformation of Medicago truncatula via infiltration of seedlings or flowering plants with Agrobacterium*. Plant J, **22**(6): 531-541.

Trinchant, J. C. and Rigaud, J. (1982). *Nitrite and nitric oxide as inhibitors of nitrogenase from soybean bacteroids*. Appl Environ Microbiol, **44**(6): 1385-1388.

Tsay, Y. F., Chiu, C. C.*, et al.* (2007). *Nitrate transporters and peptide transporters*. FEBS Lett, **581**(12): 2290-2300.

Tusnady, G. E. and Simon, I. (1998). *Principles governing amino acid composition of integral membrane proteins: application to topology prediction*. J Mol Biol, **283**(2): 489-506.

Tusnady, G. E. and Simon, I. (2001). *The HMMTOP transmembrane topology prediction server*. Bioinformatics, **17**(9): 849-850.

Tyerman, S. D., Whitehead, L. F.*, et al.* (1995). *A channel-like transporter for NH4+ on the symbiotic interface of N2-fixing plants*. Nature, **378**(6557): 629-632.

Ullrich, W. R., Larsson, M.*, et al.* (1984). *Ammonium uptake in Lemna gibba G1, related membrane potential changes, and inhibition of anion uptake*. Physiologia Plantarum, **61**(3): 369-376.

Vale, F. R., Volk, R. J.*, et al.* (1988). *Simultaneous influx of ammonium and potassium into maize roots: kinetics and interactions*. Planta, **173**(3): 424-431.

van Brussel, A. A., Recourt, K.*, et al.* (1990). *A biovar-specific signal of Rhizobium leguminosarum bv. viciae induces increased nodulation gene-inducing activity in root exudate of Vicia sativa subsp. nigra*. J Bacteriol, **172**(9): 5394-5401.

von Heijne, G. (1992). *Membrane protein structure prediction: Hydrophobicity analysis and the positive-inside rule*. Journal of Molecular Biology, **225**(2): 487-494.

Von Wirén, N., Lauter, F.-R.*, et al.* (2000). *Differential regulation of three functional ammonium transporter genes by nitrogen in root hairs and by light in leaves of tomato*. The Plant Journal, **21**(2): 167-175.

Walker, N. A., Beilby, M. J.*, et al.* (1979). *Amine uniport at the plasmalemma of charophyte cells: I. Current-voltage curves, saturation kinetics, and effects of unstirred layers*. Journal of Membrane Biology, **49**(1): 21-55.

Wallsgrove, R. M., Turner, J. C.*, et al.* (1987). *Barley mutants lacking chloroplast glutamine synthetase-biochemical and genetic analysis*. Plant Physiol, **83**(1): 155-158.

Wang, M. Y., Siddiqi, M. Y.*, et al.* (1993). *Ammonium Uptake by Rice Roots (II. Kinetics of $^{13}NH_4^+$ Influx across the Plasmalemma)*. Plant Physiol, **103**(4): 1259-1267.

Watanabe, A., Hamada, K.*, et al.* (1994). *Biphasic and differential expression of cytosolic glutamine synthetase genes of radish during seed germination and senescence of cotyledons*. Plant Molecular biology, **26**(6): 1807-1817.

Wendehenne, D., Pugin, A.*, et al.* (2001). *Nitric oxide: comparative synthesis and signaling in animal and plant cells*. Trends in Plant Science, **6**(4): 177-183.

White, P. J. (1996). *The Permeation of Ammonium through a Voltage-independent K^+ Channel in the Plasma Membrane of Rye Roots*. Journal of Membrane Biology, **152**(1): 89-99.

Yamamoto-Katou, A., Katou, S.*, et al.* (2006). *Nitrate Reductase is Responsible for Elicitin-induced Nitric Oxide Production in Nicotiana benthamiana*. Plant and Cell Physiology, **47**(6): 726-735.

Yamasaki, H., Sakihama, Y.*, et al.* (1999). *An alternative pathway for nitric oxide production in plants: new features of an old enzyme*. Trends in Plant Science, **4**(4): 128-129.

Yang, W.-C., Cramers, H. C. J. C.*, et al.* (1992). *In-situ localization of chalcone synthase mRNA in pea root nodule development*. The Plant Journal, **2**(2): 143-151.

Young, N. D., Mudge, J.*, et al.* (2003). *Legume genomes: more than peas in a pod*. Curr Opin Plant Biol, **6**(2): 199-204.

Zozaya-Hinchliffe, M., Potenza, C.*, et al.* (2005). *Nitrogen and metabolic regulation of the expression of plastidic glutamine synthetase in alfalfa (Medicago sativa)*. Plant Science, **168**(4): 1041-1052.

Zuanazzi, J. A. S., Clergeot, P. H.*, et al.* (1998). *Production of Sinorhizobium meliloti nod gene activator and repressor flavonoids from Medicago sativa roots*. Molecular Plant-Microbe Interactions, **11**(8): 784-794.

Zumft, W. G. (1997). *Cell biology and molecular basis of denitrification*. Microbiology and Molecular Biology Reviews, **61**(4): 533-616.